

149

UNH-

<p>AUTOCORRELATION AND POWER SPECTRUM ANALYSIS FOR X-RAY AND GAMMA RAY SPECTROMETER DATA</p> <p>by</p> <p>CHUNG-JEN TSAI</p> <p>M.S. Thesis</p>



FACILITY FORM 602	<u>N71-35508</u>	
	(ACCESSION NUMBER)	(THRU)
<u>88</u>		<u>G3</u>
<u>5f-121899</u>		<u>14</u>
(PAGE)		(CODE)
(NASA CR OR TMX OR AD NUMBER)		(CATEGORY)



Space Science Center
Department of Physics
UNIVERSITY OF NEW HAMPSHIRE
Durham

AUTOCORRELATION AND POWER SPECTRUM ANALYSIS
FOR X-RAY AND GAMMA RAY SPECTROMETER DATA

by

CHUNG-JEN TSAI

B. S., Cheng Kung University, Taiwan, China, 1964

A THESIS

Submitted to the University of New Hampshire

In Partial Fulfillment of

The Requirements for the Degree of

Master of Science

Graduate School

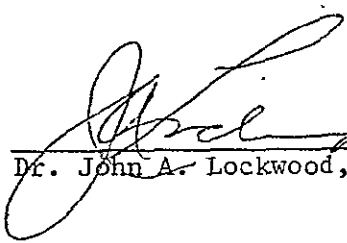
Department of Physics

June, 1971

This thesis has been examined and approved.



Thesis director, Dr. Edward L. Clapp, Prof. of Physics



Dr. John A. Lockwood, Prof. of Physics



Dr. Richard L. Kaufmann, Assoc. Prof. of Physics

25 June 1971
Date

ACKNOWLEDGMENTS

The author would like to express his gratitude to Dr. Edward L. Chupp for his guidance, encouragement, and advice throughout the work. The author would also like to thank Mr. Larry E. Orwig for his valuable suggestions. Sincere thanks are also due to Dr. John A. Lockwood and Dr. Richard L. Kaufmann for their helpful discussions.

Many thanks for Mrs. Mary M. Chupp and Mrs. Camellia I. Horne for typing the draft, and to Miss Sara Frost for her typing and assembly of the thesis.

The author is also indebted to Mr. Daniel F. Gats for his efforts in the preparation of the final version.

This research was supported by the National Aeronautics and Space Administration under contract NGL 30-002-021.

TABLE OF CONTENTS

LIST OF TABLES	vi
LIST OF FIGURES	vii
ABSTRACT	ix
I. INTRODUCTION	1
1.1 General Aim of Thesis	1
1.2 Review of Observations of Pulsar NP 0532	2
1.3 The Reasons for Using Autocorrelation and Power Spectrum Analysis for Determining the Pulsar Periods	4
1.4 Statement of Problem	5
II. THEORY	6
2.1 Theory of Autocorrelation and Power Spectrum Analysis	6
2.2 The Relation Between the Autocorrelation Function and the Power Spectrum	11
2.3 Derivation of Autocorrelation Function and Power Spectrum for Computer Programming Use	14
III. PROGRAMMING	22
3.1 The Basic Principle Used for Generating Random Data	23
3.2 Brief Statement of the Method for Generating a Square Pulse or a Pulsar Signal Including a Random Background	28
3.3 Flow Chart for Autocorrelation Function and Power Spectrum Computation	30
IV. EXAMPLE OF SIMULATED DATA	34
4.1 Autocorrelation and Power Spectrum for a Random Background	34
4.2 Autocorrelation and Power Spectrum Prediction for the Average Pulse Signal Above an Average Random Background	37
4.3 Autocorrelation and Power Spectrum Prediction for the Average Pulsar Signal Above an Average Random Background ...	43
4.4 Computer Results for the Autocorrelation Function and the Power Spectrum With Several Kinds of Simulated Data	46
1. Random Noise	46
2. Square Pulse Signal Above a Random Background	47
3. Pulsar Type Signal Above a Random Background	50
4. Smallest Detectable Pulsar Using Autocorrelation and Power Spectrum Analysis	55

V. CONCLUSION AND DISCUSSION	59
REFERENCES	62
APPENDIX A	64
APPENDIX B	67
APPENDIX C	69
APPENDIX D	79

LIST OF TABLES

1. Characteristics of NP 0532	3
2. Distribution of random time intervals	25
3. Values of autocorrelation function and power spectrum for a square pulse signal above a random background.....	51
4. Values of autocorrelation function and power spectrum for a pulsar signal above a random background	53

LIST OF FIGURES AND CAPTIONS

1.	Two identical waves without time lag	7
2.	Two identical waves with time lag	8
3.	Aliased power spectra due to folding (a) true spectra (b) ali- ased spectra	19
4.	Sampling of a sinusoidal wave	21
5.	Distribution of random time intervals	27
6.	Method of generating a square pulse or pulsar signal above a random background	29
7.	Flow chart for computing the autocorrelation function and the power spectrum	33
8.	Power spectrum and autocorrelation function for low-pass white noise	36
9.	The transformation relations between the autocorrelation func- tion and power spectrum using the autocorrelation theorem	39
10.	Predictions for average signals	40
	(a) A square pulse signal with a 100% intensity increase over the background. The mean value of signal and the background are shown.	
	(b) The square pulse signal with a 100% intensity increase over the background for a zero mean signal and back- ground.	
	(c) Normalized autocorrelation function for the data of (b)	
11.	Predictions for average signals	44
	(a) A pulsar signal with a 100% intensity increase over the background	
	(b) Pulsar signal with a 100% intensity increase over the background for a zero mean value for signal and back- ground	
	(c) Normalized autocorrelation function for the data of (b)	
12.	Computer results giving unnormalized autocorrelation functions for data of zero mean value	48
	(a) random background	
	(b) square pulse signal with 100% intensity above random background	
	(c) pulsar signal with 100% intensity above random back- ground	

13.	Computer results giving the power spectra for data of zero mean value	49
	(a) random background	
	(b) 100% intensity square pulse signal above random background	
	(c) 100% intensity pulsar signal above random background	
14.	Computer results giving the unnormalized autocorrelation function for data of zero mean value when the pulsar signal is 25% greater than the random background	56
15.	Computer results giving the power spectrum for a pulsar signal 25% greater than the random background	57
16.	Flow chart for generating random background counts	66
17.	Flow chart for generating a pulsar signal above a constant average random background counts	68

ABSTRACT

AUTOCORRELATION AND POWER SPECTRUM ANALYSIS FOR
X-RAY AND GAMMA RAY SPECTROMETER DATA

by

CHUG-JEN TSAI

The purpose of this thesis is to test the usefulness of autocorrelation and power spectrum analysis computer programs for studying signals from possible X-ray and gamma ray pulsar emitting pulsars such as NP 0532. For checking the program, simulated data are generated: (1) simulated random background, (2) simulated square pulse signal above a random background and (3) a simulated pulsar signal above a random background. These data are discrete and equally spaced time series.

The results of the analysis, when the simulated pulsar signal represents a 100% intensity increase above the random background, is in good agreement with an analytical solution. This technique fails to detect pulsar signal if it has an intensity less than 25% above the random background for a set of 10^5 data points. The sensitivity of the technique will be improved for an increased amount of data or increased observation time. Also if the period is known the parameters used in the analysis may be optimized to increase the sensitivity of the method.

CHAPTER I

INTRODUCTION

1.1 General Aim of Thesis

The emission of X-rays from the pulsar NP 0532 in the Crab Nebula has been established by the Naval Research Laboratory Group (FRIEDMAN et al., 1969) by using the autocorrelation and power spectrum analysis technique. Similarly, X-ray or gamma ray pulsations of NP 0532 could be observed by power spectrum analysis for balloon data, where flight times are several hours long and the random noise background is much larger than in rocket flights because of the atmospheric photons.

The purpose of this thesis is to test the usefulness of a computer program to calculate the autocorrelation function and power spectrum with a simulated pulsar signal superimposed on a random background. Before testing the program for calculating the autocorrelation function and power spectrum, three kinds of simulated data are generated. These are:

(1) simulated random background, (2) a simulated square pulse signal on the random background, and (3) a simulated pulsar signal on the random background. The first two are subsidiary data for checking the autocorrelation function and power spectrum computer programs.

1.2 Review of Observations of Pulsar NP 0532

Pulsars, radio-emitting "stars" having rapid and extremely accurate repetitive changes in luminosity with time, were discovered in 1968 by HEWISH, et al. (1968). Later, STAELIN and KEIFENSTEIN (1968) observed two radio pulsars in the vicinity of the Crab Nebula. Of the pulsars yet discovered, these two have the longest (3.745 s.) and shortest periods (33.09 ms.).

In January of 1969, COCKE, DISNEY, and TAYLOR (1969) reported the discovery of optical light flashes from the Crab Nebula. The flashes occurred with the same periodicity as the fast Crab pulsar (NP 0532) and were suggested to have originated south of the two central stars in the Crab Nebula.

X-ray pulsations from NP 0532 as reported by NRL (FRIEDMAN et al., 1969) indicate that it pulsates at a frequency closely matching the radio and optical pulsations. About 5% of the total average X-ray power of the Nebula appears in the pulsed component. The X-ray pulsations have the form of a main pulse and an inter-pulse, separated by about 12 ms. The important characteristics of NP 0532 (FRIEDMAN et al., 1969) for radio, optical and X-ray observations are tabulated in Table 1.

Table 1

Radio Optical X-ray			
Average Pulsed Power (erg cm ⁻² sec ⁻¹)	6×10^{-14} (195-430 Mhz)	8×10^{-12} (4500-8500A ⁰)	1.5×10^{-9} (1-10A ⁰)
Spectral Index	-2	$U-B = -1.3^*$ $B-V = +0.1$	~ 0.4
Separation of Main Pulse and Interpulse	~ 14.5 ms	14.0 ms	~ 12.0 ms
Half-power Width of Main Pulse	~ 3.0 ms	1.4 ms	≤ 2.5 ms
Half-power Width of Interpulse		3.0 ms	≤ 5.0 ms

* U, B, and V are logarithmic intensities (magnitudes) in the ultraviolet, blue, and visual, respectively.

1.3 The Reasons for Using Autocorrelation and Power Spectrum Analysis for Determining the Pulsar Periods

Autocorrelation and power spectrum analysis reveals information on pulsar characteristics in the time and frequency domain. Suppose that an X-ray or gamma ray pulsar has one pulsation period, and the intensity of the signal is strong with respect to the random background, then the autocorrelation function will be a periodic function with the same period as the signal. In the frequency domain, the power spectrum would have a large value at several definite frequencies corresponding to the pulsar's fundamental frequency, the first harmonic frequency, etc.

In general, there might be several frequencies in the pulsar in question or in other words, it might have several pulsation periods. In this situation the autocorrelation function in the lag time domain is not a good way to pick up the pulsation periods. Because the autocorrelation can be considered as the sum of the autocorrelation functions for the separate periods superimposed on the random background, the resultant autocorrelation function in the lag time domain might not be easily interpreted. On the contrary, the power spectrum allows one to easily detect those frequency components present in the pulsar. So long as this spectrum, when plotted versus frequency, has bumps or large values at several particular frequencies, one can easily tell which frequencies are the fundamental pulsation frequencies.

The power spectrum analysis determines not only the estimated value of the period but, it can determine how much power is contributed by each frequency component. The power contributed by each component is proportional to the square of the amplitude of that component.

1.4 Statement of Problem .

Knowing the actual characteristics of a typical pulsar such as NP 0532, we could simulate this data for checking the "autocorrelation and power spectrum" program. Using instead an idealized pulsar simulation we can study several questions relating to the use of autocorrelation and power spectrum analysis techniques. The basic questions studied in this thesis are: (1) what is the limitation of using the autocorrelation and power spectrum analysis techniques as the pulsar signal becomes weak compared to the background? (2) What are the various advantages and disadvantages of using the technique?

CHAPTER II

THEORY

2.1 Theory of Autocorrelation and Power Spectrum Analysis

Autocorrelation and power spectrum analysis is a very useful tool for detecting periodic signals buried in noise and for establishing coherence between random signals. Its applications range from engineering to radar and astronomy to medical, nuclear, and acoustical research.

(1) Autocorrelation Function

Autocorrelation for any kind of waveform is a measure of the reinforcement between two identical waveforms shifted in phase. It is computed by multiplying one waveform ordinate by ordinate with the other and finding the average value of the product. If there is no phase shift involved, the correlation between two identical waveforms is large. In other words, the autocorrelation function at the zero lag time is large and a maximum. However, if two waveforms are identical in shape but have an arbitrary time shift between them, then the correlation between them is generally small. Hence, autocorrelation is a function of the time shift between the two identical waveforms. This correlation problem is illustrated in Figures 1 and 2. Figure 1 shows two identical waveforms without any time lag or phase shift. Figure 2 illustrates two identical waveforms with a lag time or phase shift.

This function can be expressed in terms of a mathematical formula as the product of the wave $x(t)$ and a delayed version of itself $x(t + \tau)$ aver-

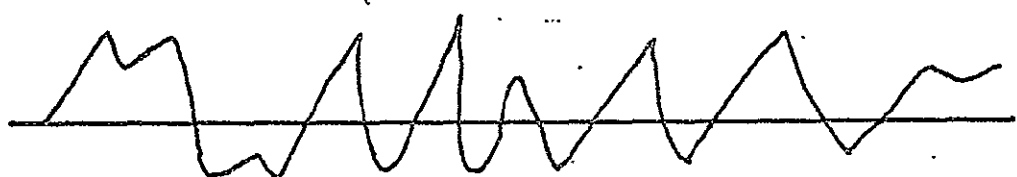
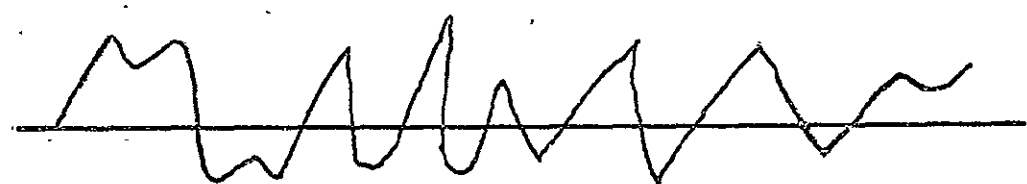


FIGURE 1

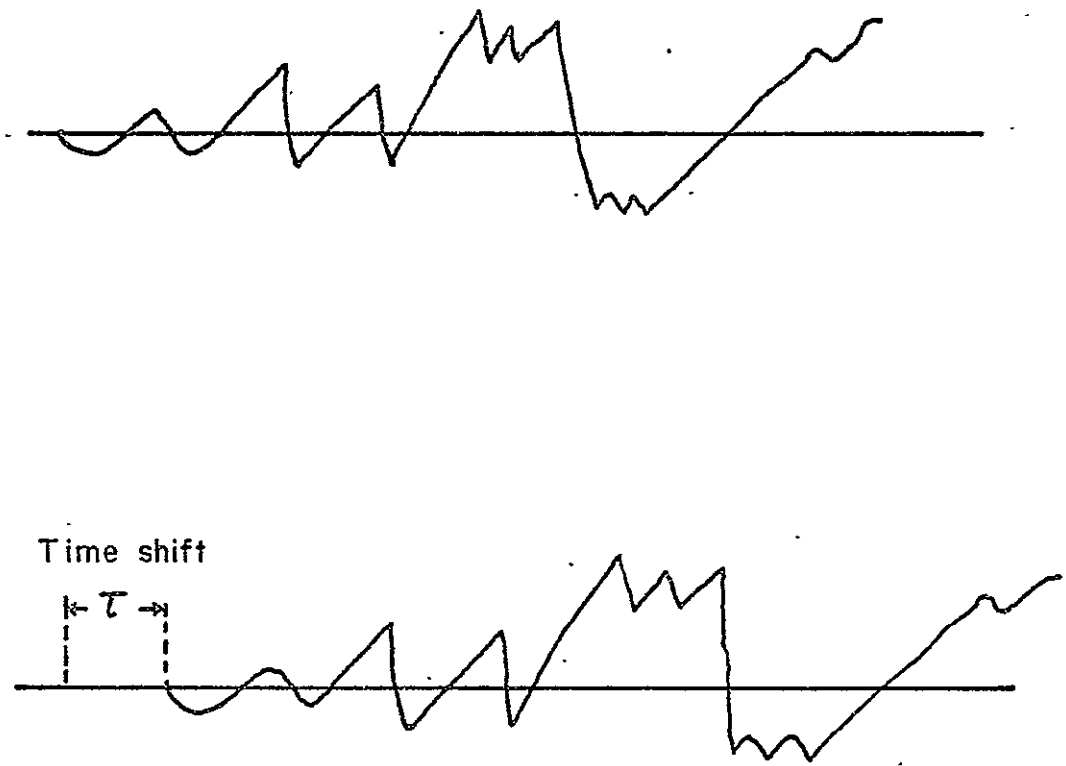


FIGURE 2

aged over T seconds as follows:

$$R(\tau) = \lim_{T \rightarrow \infty} \frac{1}{T} \int_0^T x(t) x(t + \tau) dt \quad (1)$$

where τ is the lag time. This quantity $R(\tau)$ is always a real-valued even function with a maximum at $\tau=0$ and may be either positive, negative or zero for other values of τ . There may be other maxima depending on the function. Therefore, this function has:

1. Symmetry about $\tau=0$, i.e. $R(\tau) = R(-\tau)$ (2)

2. A maximum at $\tau=0$ equal to the mean square value (\bar{x}^2) (3)

of the signal from which it is derived, i.e. $R(0) = \bar{x}^2$

and $R(0) \geq R(\tau)$ for all τ .

Also for the special case of a periodic waveform the autocorrelation function is periodic and has the same period as the waveform itself. This periodic autocorrelation has the two properties listed above but it will have maxima whenever the lag time τ is equal to an integral number of periods of the signal.

The random noise signal is quite different from the periodic waveform. When compared with a time shifted version of itself, only a small time shift is required to destroy the correlation, and it never recurs. The autocorrelation function for this case is, therefore, a sharp impulse which decays from the central maximum to low values at large time shifts.

Two samples of random noise of the same bandwidth might have quite different waveforms, but their autocorrelation functions could be identical. The autocorrelation function of any signal, random or periodic, depends not on the actual waveform but on its frequency content.

(2) Power Spectrum

The power spectral density function at frequency f_c is defined by BENDAT (1958) as:

$$G(f_c, x) = \lim_{\Delta f \rightarrow 0} \frac{P(f_c, x, \Delta f)}{\Delta f} \quad (4)$$

where $P(f_c, x, \Delta f)$ is the total average power in a given bandwidth Δf and x is a continuous variable. Therefore, the above equation represents the limit of the total average power in a given bandwidth divided by the bandwidth as the bandwidth approaches zero. Suppose $x(t)$ represents an infinite record length, then we can define data with a finite record length as:

$$x_T(t) = \begin{cases} x(t) & |t| \leq T \\ 0 & \text{otherwise} \end{cases}$$

The total average power of bandwidth Δf is defined by BENDAT (1958) as:

$$P(f_c, x, \Delta f) = \lim_{T \rightarrow \infty} \int_{f_c - \frac{\Delta f}{2}}^{f_c + \frac{\Delta f}{2}} \frac{|A_T(f, x)|^2}{T} df \quad (5)$$

where

$$A_T(f, x) = \int_{-T}^T x(t) e^{-i2\pi ft} dt = \int_{-\infty}^{\infty} x_T(t) e^{-i2\pi ft} dt \quad (6)$$

$A_T(f, x)$ is the direct Fourier transformation of the finite length of data $x_T(t)$ and

$$|A_T(f, x)|^2 = A_T^*(f, x) A_T(f, x) \quad (7)$$

From equations (4) and (5) we observe that since $|A_T(f, x)|^2$ is an even function of f , it follows that $G(f, x)$ is an even function for all f . The notation $G(f, x)$ shows clearly that the power spectral density function depends upon the particular time record $x(t)$ under examination.

2.2 The Relation Between the Autocorrelation Function and the Power Spectrum

Consider an arbitrary real-valued time record $x(t)$ of infinite extent. Its total energy is defined by

$$\text{Total energy} = \int_{-\infty}^{\infty} x^2(t) dt \quad (8)$$

If $x(t)$ does not approach zero rapidly enough for large values of t , the total energy may be infinite; that is, this integral fails to converge. However, we shall assume that the average power associated with $x(t)$ is finite, where the average power is defined by

$$P_{av} = \lim_{T \rightarrow \infty} \frac{1}{2T} \int_{-T}^{T} x^2(t) dt \quad (9)$$

Using Parseval's Theorem as given by KHARKEVICH (1960a), let $A_1(f, x_1)$ and $A_2(f, x_2)$ be the Fourier transformation of real functions $x_1(t)$ and $x_2(t)$, respectively. Then

$$\int_{-\infty}^{\infty} x_1(t) x_2(t) dt = \int_{-\infty}^{\infty} A_1^*(f, x_1) A_2(f, x_2) df \quad (10)$$

For the special case of $x_1(t) = x_2(t)$ and a finite record

$$\int_{-\infty}^{\infty} x_T^2(t) dt = \int_{-\infty}^{\infty} |A_T(f, x)|^2 df = 2 \int_0^{\infty} |A_T(f, x)|^2 df \quad (11)$$

If $\int_{-\infty}^{\infty} x_T^2(t) dt$ is convergent, then by (11)

$$P_{av} = \lim_{T \rightarrow \infty} \frac{1}{2} \int_{-\infty}^{\infty} \frac{x_T^2(t)}{T} dt = \lim_{T \rightarrow \infty} \int_0^{\infty} \frac{|A_T(f, x)|^2}{T} df \quad (12)$$

Therefore, from equations (3), (4), (5), (11) and (12)

$$R(0) = \bar{X^2}(t) = \lim_{T \rightarrow \infty} \frac{1}{2T} \int_{-T}^T X^2(t) dt = \int_0^\infty G(f) df \quad (13)$$

but

$$R(0) = \int_{-\infty}^\infty R(\tau) \delta(\tau) d\tau = 2 \int_0^\infty R(\tau) \delta(\tau) d\tau$$

because $R(\tau)$ and $\delta(\tau)$ are even functions.

Therefore, by use of the definition of the Dirac delta function $\delta(\tau)$

$$R(0) = 2 \int_0^\infty R(\tau) \int_{-\infty}^\infty e^{-i2\pi f\tau} df d\tau \quad (14)$$

Comparing (13) and (14)

$$G(f) = 2 \int_{-\infty}^\infty R(\tau) e^{-i2\pi f\tau} d\tau$$

Therefore, the power spectrum is the Fourier transform of the autocorrelation function. The power spectrum can be written in another form as follows

$$G(f) = 4 \int_0^\infty R(\tau) \cos 2\pi f \tau d\tau$$

Since $R(\tau)$ is an even function of τ , $G(f)$ is always a real-valued non-negative function. In short, the autocorrelation function and power spectrum are the Fourier transformation pair, i.e.,

$$R(\tau) = \int_0^\infty G(f) \cos 2\pi f \tau df \quad (15)$$

$$G(f) = 4 \int_0^\infty R(\tau) \cos 2\pi f \tau d\tau$$

Autocorrelation Theorem

There is a useful theorem which is stated by BRACEWELL (1965) and can be used to explain the relation between power spectrum and autocorrelation function. If $X(t)$ has the Fourier transform $A(f)$, then its auto-

correlation function is the Fourier transform of $|A(f)|^2$. i.e., if

$$\int_{-\infty}^{\infty} X(t) e^{-i 2\pi f t} dt = A(f)$$

then,

$$\int_{-\infty}^{\infty} |A(f)|^2 e^{i 2\pi f \tau} df = \int_{-\infty}^{\infty} X^*(t) X(t + \tau) dt \quad (16)$$

This autocorrelation function is unnormalized with zero mean. Thus $|A(f)|^2$ is the power spectrum in equation (16), since the Fourier transformation of the autocorrelation function is the power spectrum, that is

$$\int_{-\infty}^{\infty} R(\tau) e^{-i 2\pi f \tau} d\tau = G(f)$$

Conversely, the autocorrelation function is the Fourier transform of $G(f)$

$$\int_{-\infty}^{\infty} G(f) e^{i 2\pi f \tau} df = R(\tau) = \int_{-\infty}^{\infty} X^*(t) X(t + \tau) dt$$

from the above equation compared with equation (16) we see that $|A(f)|^2$ is equal to $G(f)$.

2.3 Derivation of Autocorrelation Function and Power Spectrum
for Computer Programming Use

The functions used in the first two sections of this chapter were continuous for the convenience of the theoretical treatment. In practice digital type data are normally used. For example, the data obtained by collecting counts over some time interval Δt is discrete. Therefore, in this sense, the simulated data we must use should be discrete.

The simulated data will be equi-spaced, discrete and for a finite length record. For this reason, the formulas of autocorrelation function and power spectrum must be transformed.

Suppose this series of data has a non-zero mean. An estimated autocorrelation function [I.B.M. Programmer's Manual: System/360 Scientific Subroutine Package, (360A - CM 03X), Version III, 59.] may be expressed as

$$\hat{R}_j = \frac{1}{n-j+1} \sum_{i=1}^{n-j+1} (X_i - \bar{X})(X_{i+j-1} - \bar{X}) \quad (17)$$

where:

\bar{X} is the mean value of all the data X_i , i.e. $\bar{X} =$
 n = number of observations in the time series X_i
 $j = 1, 2, 3, \dots, m$ represents time lags 0, 1, 2, ..., $(m-1)$ and
 m is the maximum lag number and the maximum lag time $T_m = (m-1) \times$ sampling time. For programming convenience, we may expand equation (17) into three terms as follows:

$$\hat{R}_j = \frac{1}{n-j+1} \left[\sum_{i=1}^{n-j+1} X_i X_{i+j-1} - \bar{X} \sum_{i=1}^{n-j+1} (X_i + X_{i+j-1}) + \sum_{i=1}^{n-j+1} (\bar{X})^2 \right] \quad (18)$$

The middle term can be expressed differently by using \bar{X} according to the mathematical steps following:

$$\begin{aligned}\bar{X} &= \frac{1}{n} \sum_{i=1}^n x_i = \frac{1}{n} \left(\sum_{i=1}^{n-j+1} x_i + \sum_{i=n-j+2}^n x_i \right) \\ \therefore \sum_{i=1}^{n-j+1} x_i &= n\bar{X} - \sum_{i=n-j+2}^n x_i \quad (19)\end{aligned}$$

and $\sum_{i=1}^{n-j+1} x_{i+j-1} = \sum_{k=j}^n x_k = \sum_{i=j}^n x_i$

but $\bar{X} = \frac{1}{n} \sum_{i=1}^n x_i = \frac{1}{n} \left(\sum_{i=1}^{j-1} x_i + \sum_{i=j}^n x_i \right)$

$$\therefore \sum_{i=1}^{n-j+1} x_{i+j-1} = \sum_{i=j}^n x_i = n\bar{X} - \sum_{i=1}^{j-1} x_i \quad (20)$$

From equation (19) and equation (20)

$$\sum_{i=1}^{n-j+1} (x_i + x_{i+j-1}) = 2n\bar{X} - \left(\sum_{i=1}^{j-1} x_i + \sum_{i=n-j+2}^n x_i \right) \quad (21)$$

Substituting equation (21) in equation (18) gives the autocorrelation function with non-zero mean as follows

$$\begin{aligned}R_j &= \frac{1}{n-j+1} \left\{ \sum_{i=1}^{n-j+1} x_i x_{i+j-1} - \bar{X} \left[2n\bar{X} - \left(\sum_{i=1}^{j-1} x_i + \sum_{i=n-j+2}^n x_i \right) \right] \right. \\ &\quad \left. + (n-j+1) \bar{X}^2 \right\} \\ &= \frac{1}{n-j+1} \left[\sum_{i=1}^{n-j+1} x_i x_{i+j-1} + \bar{X} \left(\sum_{i=1}^{j-1} x_i + \sum_{i=n-j+2}^n x_i \right) - (n-j+1) \bar{X}^2 \right] \quad (22)\end{aligned}$$

Equation (22) is the complete expression for calculating the autocorrelation function with a non-zero mean for equi-spaced, discrete data. The

parenthesis of the second term of this equation is the total sum of the first $(j-1)$ data samples and the sum of the last $(j-1)$ data samples.

BLACKMAN AND TUKEY (1958a), states that the ensemble average of the estimated autocorrelation function for the discrete case equals the true autocorrelation function for the continuous case. So that

$$\text{ave} \{ \hat{R}_j \} = R(\tau) = R(j\Delta\tau)$$

Similarly, the average of the raw power spectral density can be expressed in the form of a Fourier transform, viz.,

$$\text{ave} \{ \hat{G}_K \} = 2 \int_{-\infty}^{\infty} [\nabla_m(\tilde{\tau}; \Delta\tilde{\tau}), R(\tilde{\tau})] e^{-i2\pi f \tilde{\tau}} d\tilde{\tau}$$

where $\nabla_m(\tau; \Delta\tau)$ is a finite Dirac comb, viz.,

$$\nabla_m(\tilde{\tau}; \Delta\tilde{\tau}) \equiv \frac{\Delta\tilde{\tau}}{2} \delta(\tilde{\tau} + m\Delta\tilde{\tau}) + \Delta\tilde{\tau} \sum_{j=-m+1}^{j=m-1} \delta(\tilde{\tau} - j\Delta\tilde{\tau}) + \frac{\Delta\tilde{\tau}}{2} \delta(\tilde{\tau} - m\Delta\tilde{\tau})$$

$$\begin{aligned} \text{Then } \text{ave} \{ \hat{G}_K \} &= 2 \int_{-\infty}^{\infty} \frac{\Delta\tilde{\tau}}{2} \delta(\tilde{\tau} + m\Delta\tilde{\tau}) R(\tilde{\tau}) \cos 2\pi f \tilde{\tau} d\tilde{\tau} + \\ &2\Delta\tilde{\tau} \int_{j=-m+1}^{j=m-1} \sum \delta(\tilde{\tau} - j\Delta\tilde{\tau}) R(\tilde{\tau}) \cos 2\pi f \tilde{\tau} d\tilde{\tau} + \Delta\tilde{\tau} \int_{-\infty}^{\infty} \delta(\tilde{\tau} - m\Delta\tilde{\tau}) R(\tilde{\tau}) \\ &\cos 2\pi f \tilde{\tau} d\tilde{\tau} \\ &= 2\Delta\tilde{\tau} R(m\Delta\tilde{\tau}) \cos 2\pi f m\Delta\tilde{\tau} + 2\Delta\tilde{\tau} R(0) + 4\Delta\tilde{\tau} \sum_{j=1}^{m-1} R(j\Delta\tilde{\tau}) \cos 2\pi f j\Delta\tilde{\tau} \\ &= 2\Delta\tilde{\tau} \text{ave} \{ \hat{R}_m \} \cos 2\pi f m\Delta\tilde{\tau} + 2\Delta\tilde{\tau} \text{ave} \{ \hat{R}_0 \} + 4\Delta\tilde{\tau} \sum_{j=1}^{m-1} \text{ave} \{ \hat{R}_j \} \\ &\cos 2\pi f j\Delta\tilde{\tau} \end{aligned}$$

If we ignore the averaging (Ave) in the above equation, the raw spectral density may be expressed as:

$$\hat{G}_K = 2\Delta\tilde{\tau} \hat{R}_m \cos 2\pi f m\Delta\tilde{\tau} + 2\Delta\tilde{\tau} \hat{R}_0 + 4\Delta\tilde{\tau} \sum_{j=1}^{m-1} \hat{R}_j \cos 2\pi f j\Delta\tilde{\tau} \quad (23)$$

where f is not a continuous variable any more but is now a discrete particular number.

Let

$$2\pi f_K j \Delta \tilde{\tau} = \frac{j K \pi}{m} \quad \text{i.e.,} \quad f_K = \frac{K}{2m \Delta \tilde{\tau}} \quad (24)$$

where $K = 0, 1, 2, \dots, m$

Then equation (23) becomes,

$$\tilde{G}_K = 2\Delta \tilde{\tau} \left[\hat{R}_0 + 2 \sum_{j=1}^{m-1} \hat{R}_j \cos \frac{j K \pi}{m} + (-1)^K \hat{R}_m \right] \quad (25)$$

In order to get a smoothed power spectrum the lag window and the spectral window are involved. The lag window is the Fourier transform of the spectral window. There are several Fourier transformation pairs (BLACKMAN and TUKEY, 1958b) relating these two windows: in the following D denotes lag window and Q denotes spectral window.

Zeroth pair

$$\begin{aligned} D_0(\tilde{\tau}) &= 1 & |\tilde{\tau}| < T_m \\ &= 0 & |\tilde{\tau}| > T_m \end{aligned}$$

and

$$Q_0(f) = 2T_m \frac{\sin 2\pi f T_m}{2\pi f T_m}$$

First pair (BARTLETT, 1950)

$$\begin{aligned} D_1(\tilde{\tau}) &= 1 - \frac{|\tilde{\tau}|}{T_m} & |\tilde{\tau}| < T_m \\ &= 0 & |\tilde{\tau}| > T_m \end{aligned}$$

and

$$Q_1(f) = T_m \left(\frac{\sin 2\pi f T_m}{\pi f T_m} \right)^2$$

Second pair (sometimes called "Hanning")

$$\begin{aligned} D_2(\tilde{\tau}) &= \frac{1}{2} \left(1 + \cos \frac{\pi \tilde{\tau}}{T_m} \right) & |\tilde{\tau}| < T_m \\ &= 0 & |\tilde{\tau}| > T_m \end{aligned}$$

and

$$Q_2(f) = \frac{1}{2} Q_0(f) + \frac{1}{4} \left[Q_0(f + \frac{1}{2T_m}) + Q_0(f - \frac{1}{2T_m}) \right]$$

Third pair (sometimes called "Hamming")

$$\begin{aligned} D_3(\tilde{\tau}) &= 0.54 + 0.46 \cos \frac{\pi \tilde{\tau}}{T_m} & |\tilde{\tau}| < T_m \\ &= 0 & |\tilde{\tau}| > T_m \end{aligned}$$

and

$$Q_3(\tilde{\tau}) = 0.54 Q_0(f) + 0.23 \left[Q_0(f + \frac{1}{2T_m}) + Q_0(f - \frac{1}{2T_m}) \right]$$

Fourth pair

$$D_4(\tau) = \begin{cases} 0.42 + 0.50 \cos \frac{\pi \tau}{T_m} + 0.08 \cos \frac{2\pi \tau}{T_m} & |\tau| < T_m \\ 0 & |\tau| > T_m \end{cases}$$

and

$$Q_4(\tau) = 0.42 Q_0(f) + 0.25 \left[Q_0(f + \frac{1}{2T_m}) + Q_0(f - \frac{1}{2T_m}) \right] \\ + 0.04 \left[Q_0(f + \frac{1}{T_m}) + Q_0(f - \frac{1}{T_m}) \right]$$

BENDAT and PIERSOL (1966a) use Hanning (second pair) for smoothing the raw power spectrum.

The smoothed power spectrum is the convolution of $Q_2(f)$ and the true power spectrum. Therefore

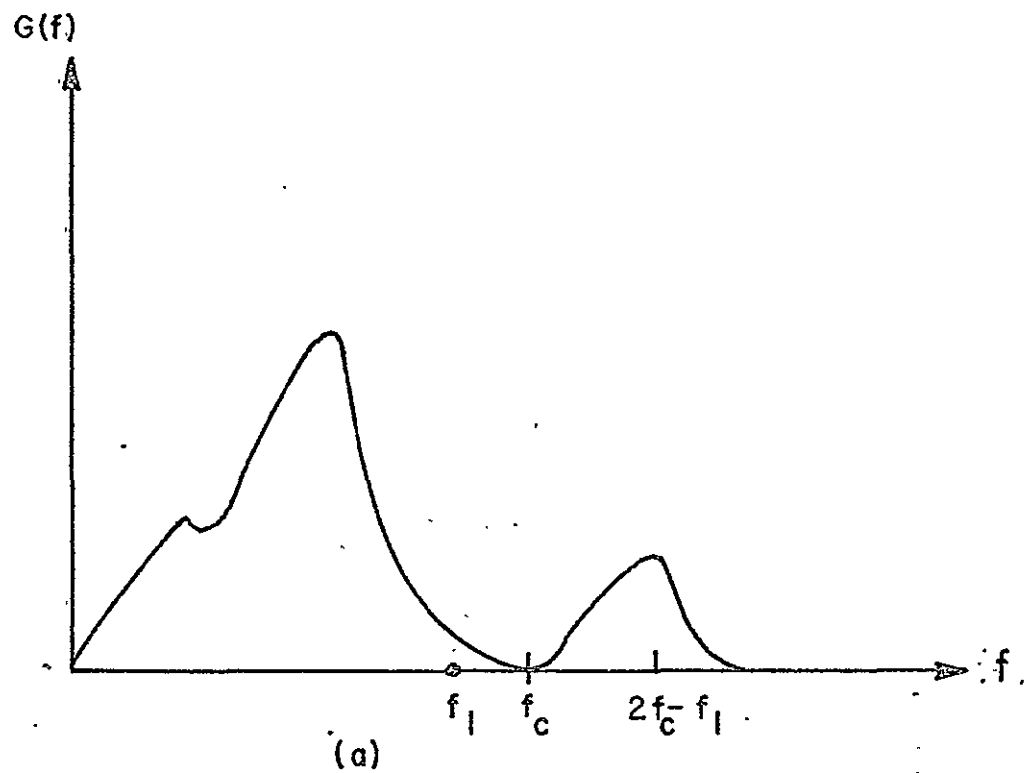
$$\hat{G}_0 = 0.5 \tilde{G}_0 + 0.5 \tilde{G}_1$$

$$\hat{G}_K = 0.25 \tilde{G}_{K-1} + 0.5 \tilde{G}_K + 0.25 \tilde{G}_{K+1} ; \quad K=1, 2, \dots, m-1 \quad (26)$$

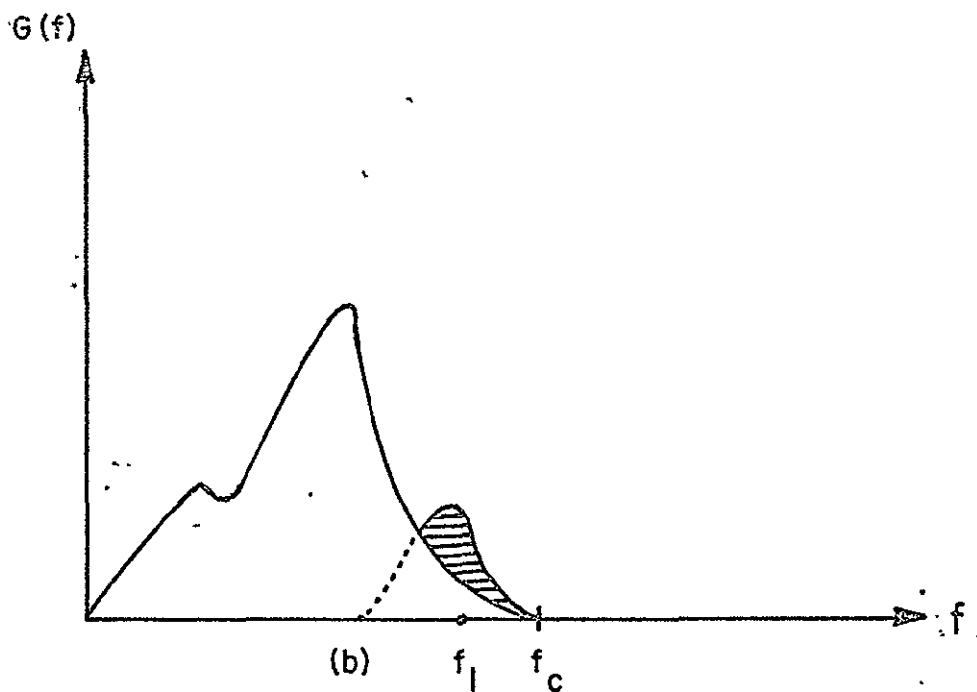
$$\hat{G}_m = 0.5 \tilde{G}_{m-1} + 0.5 \tilde{G}_m$$

KHARKEVICH (1960b) states that, "Any function $f(t)$ consisting only of frequencies from 0 to f_c can, with any desired accuracy be treated as a succession of numbers recurring every $\frac{1}{2f_c}$ seconds." Where f_c in the notation of BLACKMAN and TUKEY is f_n . This maximum frequency is also known as the folding (or Nyquist) frequency. From the equation (24), when K equals m then $f_c = \frac{1}{2\Delta\tau}$ which is the Nyquist frequency. $\Delta\tau$ in the notation of BENDAT and PIERSOL (1966b) is h or the time interval between samples. The resolution bandwidth for power spectrum is defined as $B = \frac{1}{mh}$. The B will be small for a given h when m is large.

An important feature known as "aliasing" enters for observing an equally spaced, discrete finite record of data. The energy or power at an arbitrary frequency f cannot in general be separated from that contributed by different frequencies [BLACKMAN and TUKEY (1958c)]. In other words, higher frequencies from the original process $G(f)$ may contribute some power to the estimated power spectrum $G_A(f)$ (see Fig. 3). Figures 3a and 3b in-



(a)



(b)

FIGURE 3

dicate that the powers contributed by frequencies $2f_c - f_1$ and f_1 are indistinguishable. The essential, unavoidable nature of this problem is made clear by Fig. 4 which illustrates how equally spaced time samples from any cosine wave could have come from each of many other cosine waves. In Fig. 4, the sampling time $\Delta\tau$ is 0.2 second; then the Nyquist frequency is $\frac{1}{2\Delta\tau} = \frac{1}{0.4}$ cycle/sec., i.e., 2.5 cycle/sec. Clearly, a sinusoidal wave with frequency 4 cycle/sec. can be fit through the points and a second sinusoidal wave (dotted curve) with a frequency 1 cycle/sec may also fit the given points. Higher frequencies may also be present but it is not possible to know from the measured $\Delta\tau$ whether the power at frequency f [of a power spectrum in the interval $(0, f_c)$] comes from the principal frequency f or $2f_c - f$, $sf_c + f$, $4f_c - f$, $4f_c + f$,etc. These higher frequencies are called aliases of f . Therefore, the aliased power spectrum $G_A(f)$ defined in the interval $(0, f_c)$ by BLACKMAN and TUKEY (1958d) is all that one may estimate from the data.

$G_A(f)$ may be represented as follows:

$$G_A(f) = G(f) + G(2f_c - f) + G(2f_c + f) + \dots \text{etc. } 0 \leq |f| \leq f_c$$

$$G_A(f) = 0$$

where $G(f)$ is the true power spectrum.

Two practical methods exist for handling this aliasing problem [BENDAT and PIERSOL (1966c)]. The first method is to choose h sufficiently small so that it is physically unreasonable for data to exist above the associated Nyquist frequency f_c . For the low frequency case of interest, say below 500 HZ., then $h = 1$ ms would technically be sufficient. The second method is to filter the data prior to sampling so that no information above the Nyquist frequency is contained in the filtered data. Then choosing f_c as the maximum frequency of interest will give accurate results for frequencies below f_c .

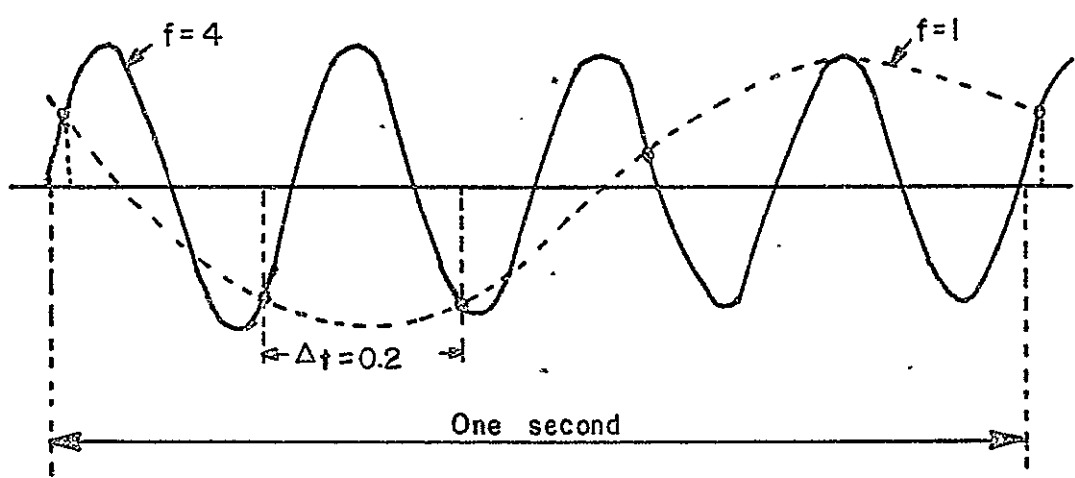


FIGURE 4

CHAPTER III

PROGRAMMING

The X-ray or Gamma ray spectrum of a pulsar might be in the form of a small signal on the random background. Autocorrelation and power spectrum analysis has already been used as a tool in conjunction with a rocket experiment (NRL Group) for detecting the X-ray pulsar (NP 0532) signal over the general Crab X-ray signal. Similarly, the autocorrelation and power spectrum technique might be used for balloon experiments. In order to check the programs for computing the autocorrelation and power spectral density function before applying them to balloon flight data, three kinds of simulated data are generated by the computer. The first one is a simulated random background for discrete data. The second one is a simulated square pulse signal above a random background. The third one is a simulated pulsar signal above the random background.

3.1 The Basic Principle Used for Generating Random Data

A way of generating random data is to use the time interval distribution which is derived from the Poisson distribution which gives the probability distribution in time for a random process when the average rate is specified.

The time interval distribution describes the distribution in size of the time intervals between successive random counts when the mean rate has the constant value of \bar{a} counts per unit time. From EVANS (1955) suppose \bar{a} is the average rate of appearance of photons; then the average number of counts in a time interval t is \bar{at} .

When the average rate is \bar{a} , the probability of observing x counts in a time interval t can be expressed as follows:

$$P_x(t) = \frac{(\bar{at})^x}{x!} e^{-\bar{at}}$$

This is simply the Poisson Distribution. From this equation the probability that there will be no counts in a time interval t , during which time there should be \bar{at} counts on the average, is

$$P_0 = \frac{(\bar{at})^0}{0!} e^{-\bar{at}} = e^{-\bar{at}}$$

and its differential form is shown as follows:

$$\left| \frac{dP_0}{dt} \right| = \bar{a} e^{-\bar{at}}$$

We at once see that small time intervals between successive random counts have a higher probability (probability of no counts in a time interval t) of occurring than large time intervals. In other words, this is the TIME INTERVAL DISTRIBUTION which gives the probability of occurrence of each time interval.

Of course, the occurrence of a given time interval is random and may be represented by a random number. This implies that the differential probability of occurrence of a given time interval may also be represented by a random number.

Now from the random time interval between two successive counts, the random counts within a definite time interval could be generated. Those random counts are the simulated data I have been using. Suppose all events (counts) occur randomly along a time axis, the number of random counts is then nothing but the number of counts occurring within a definite time interval.

Thus, the steps of generating random counts is shown as follows:

1. Generate random number between 0 and 1 by use of the SUBROUTINE 'RANDU.' (see Appendix A)
2. Take this random number as the probability of no counts occurring in a time interval t_i but one count in t_i to $t_i + dt_i$ and generate random time intervals according to the formula $t_i = -\frac{\ln \text{UNIT}}{\bar{a}}$; where t_i is a random time interval and UNIT is random number between 0 and 1.
3. Generate the number of random counts within a given desired sampling time by observing the sequence of intervals obtained from step 2. The distribution of the random time intervals is shown in Figure 5 by using some of the data from the "Random Data" program. The random time interval data have been generated under the average counting rate $\bar{a}=1$ count/ms. The total number of random time intervals is 1.5×10^5 , but only 1.5×10^4 are printed out with the form of 1500 numbers of random time intervals for each 10th record. In other words, there are 1500 numbers of random time intervals for 10th, 20th, 30th up to 100th record.

In order to show the distribution of time intervals, the grouping of the numbers of time interval in the range of $0 \sim 0.1$ ms, $0.1 \sim 0.2$ ms, etc. is tabulated in Table 2.

Table 2

Range of Time Interval (ms)	Numbers of Time Interval (counts)	Total Number (Counts)
0.1 ~ 0.2	150	
0.2 ~ 0.3	110	
0.3 ~ 0.4	102	
0.4 ~ 0.5	84	
0.5 ~ 0.6	82	
0.6 ~ 0.7	72	
0.7 ~ 0.8	62	1173
0.8 ~ 0.9	46	
0.9 ~ 1.0	62	
1.0 ~ 1.1	50	
1.1 ~ 1.2	59	
1.2 ~ 1.3	41	
1.3 ~ 1.4	38	
1.4 ~ 1.5	33	
1.5 ~ 1.6	37	
1.6 ~ 1.7	27	
1.7 ~ 1.8	40	
1.8 ~ 1.9	24	
1.9 ~ 2.0	17	
2.0 ~ 2.1	21	
2.1 ~ 2.2	16	

There are only 1173 out of 1500 values of time intervals taken from the first 1500 values of printed data from the program of "Generating Random Data."

Figure 5 is a semilogarithmic plot of the numbers of time intervals in a given sampling time of 1 ms versus the time interval. The straight line shows that the distribution is exponential as we expect. From the slope of the line, we can determine \bar{a} for checking the "Random Data" program.

As I mentioned above $\bar{a} = 1$ count/ms gives 1 count within 1 ms on the average which is a very low value statistically. Therefore the distribution of x counts occur within 1 ms time interval will follow the Poisson distribution $P_x(t) = \frac{(\bar{a}t)^x}{x!} e^{-\bar{a}t}$. Substituting this value in this equation, then $P_x(1) = \frac{1}{x!} e^{-1}$; where $P_x(1)$ is a random number because of x random counts. The slope of the straight line in Fig. 5 is 1.17 cts/ms. The 17% error is due to the limited data (1173), this would decrease with more data. A least square fit may give a better result.

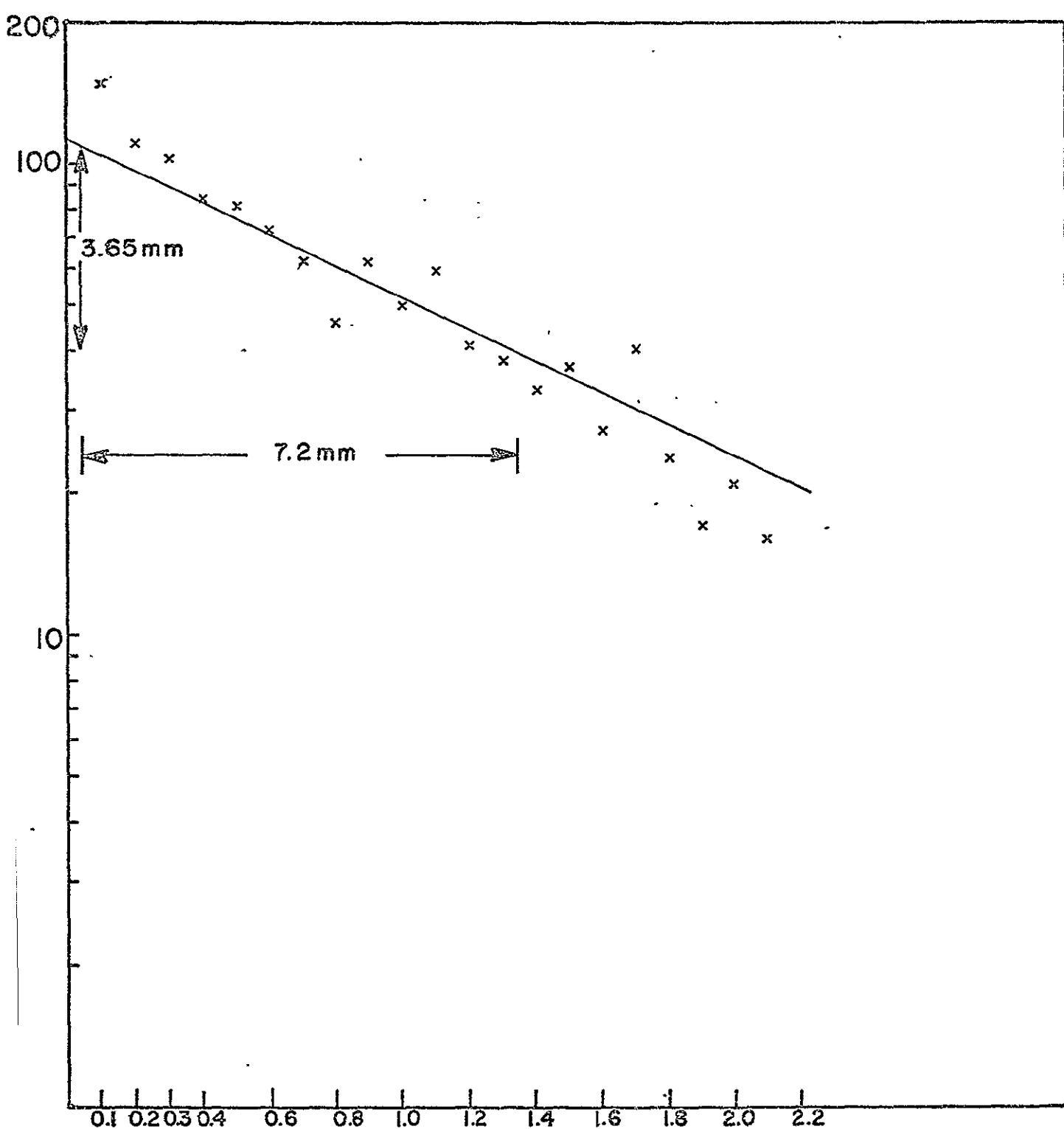


FIGURE 5

3.2 Brief Statement of the Method for Generating a Square Pulse or a Pulsar Signal Including a Random Background

From Section 3.1, we know that the random background has been generated by three steps. Once the random background has been generated, the random counts for either the square pulse or pulsar signal also could be generated by the same steps.

The process of constructing simulated data can be understood by reference to Figure 6. This shows the case where in region I the random counts correspond to an average rate \bar{a} and are generated by the method described in Section 3.1. In region II, the random counts are generated for a new average rate f times the former rate, where f is any positive real number. To construct the data for a continuous flow of time, the random counts for \bar{a} are used for a time t_1 , and then for a time t_2 the random counts for the new average, $f\bar{a}$, are used, then the counts for \bar{a} again for t_1 are used etc. This procedure constructs the time series for a pulse which is on for a time t_2 and off for a time t_1 so the period is $t_1 + t_2$.

If we set $t_1 = t_2 = 20$ ms, and $\bar{a} = 1$ ct/ms, and $f\bar{a} = 2$ cts/ms, then the data would be the square pulse with a 100% intensity increase over the random background with period 40 ms. Similarly, a pulsar signal with a period of 40 ms and a 100% intensity above the random background could be generated in the same way by setting $t_1 = 35$ ms, $t_2 = 5$ ms, $\bar{a} = 1$ ct/ms, and $f\bar{a} = 2$ cts/ms.

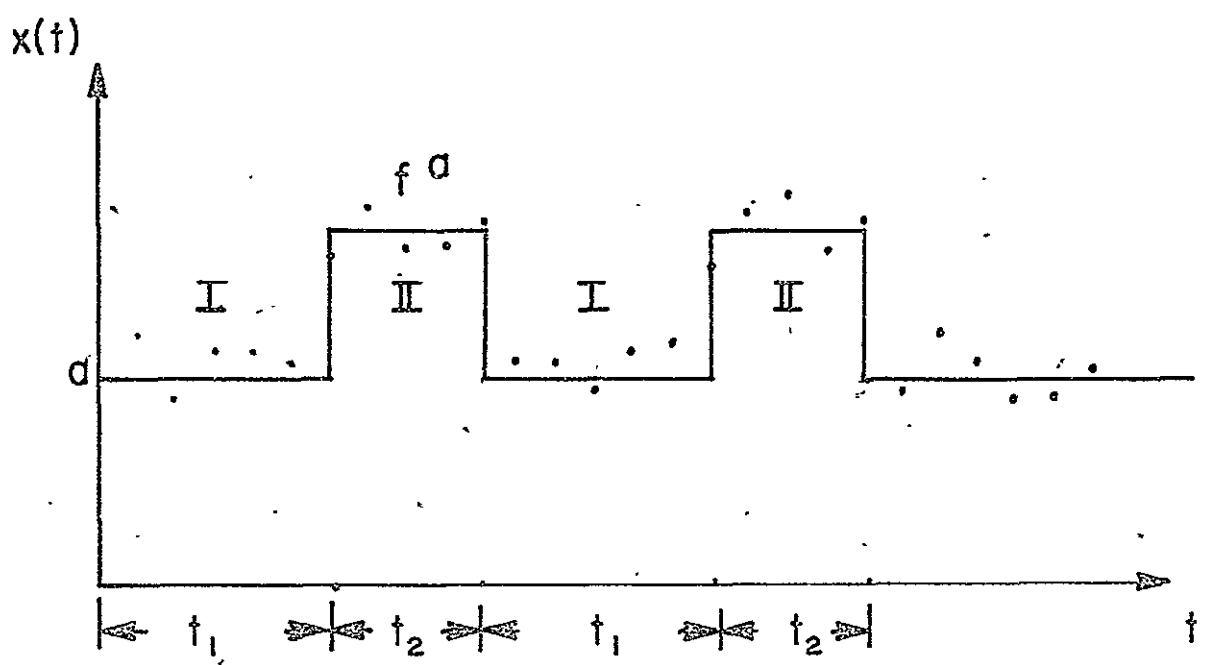


FIGURE 6

3.3 Flow Chart for Autocorrelation Function and Power Spectrum Computation

We will now discuss the procedure for developing programs to calculate the autocorrelation function and power spectrum. It is most convenient to describe this in terms of a flow chart.

The autocorrelation function with nonzero mean for discrete data is given by

$$R_j = \frac{1}{n-j+1} \sum_{i=1}^{n-j+1} (x_i - \bar{x})(x_{i+j-1} - \bar{x}) \quad (17)$$

where \bar{x} is the mean value of the data x_i ,

$$\bar{x} = \frac{1}{n} \sum_{i=1}^n x_i$$

n = number of observation in time series x_i

$j = 1, 2, 3, \dots, m$ represents time lags 0, 1, 2, ..., $(m-1)$

The transformed equation

$$\hat{R}_j = \frac{1}{n-j+1} \left[\sum_{i=1}^{n-j+1} x_i x_{i+j-1} + \left(\sum_{i=1}^{j-1} x_i + \sum_{i=n-j+2}^n x_i \right) \bar{x} - (n+j-1) \bar{x}^2 \right] \quad (22)$$

The raw power spectral density function

$$\widetilde{G}_K(f) = \widetilde{G}\left(\frac{Kf_c}{m}\right) = 2h \left[\hat{R}_0 + 2 \sum_{j=1}^{m-1} \hat{R}_j \cos\left(\frac{\pi j K}{m}\right) + (-1)^K \hat{R}_m \right] \quad (25)$$

where $f = \frac{Kf_c}{m}$. $K = 0, 1, 2, \dots, m$

h is the sampling time interval

\hat{R}_j is the estimate of the autocorrelation function at time lag $j-1$

m is the maximum lag number

$f_c = \frac{1}{2h}$ is the Nyquist frequency

The smoothed power spectrum is given by

$$\begin{aligned}\hat{G}_0 &= 0.5 \tilde{G}_0 + 0.5 \tilde{G}_1 \\ \hat{G}_k &= 0.25 \tilde{G}_{k-1} + 0.5 \tilde{G}_k + 0.25 \tilde{G}_{k+1} ; \quad k=1, 2, \dots, m-1 \\ \hat{G}_m &= 0.5 \tilde{G}_{m-1} + 0.5 \tilde{G}_m\end{aligned}\quad (26)$$

It is very cumbersome to calculate the autocorrelation function throughout all the data. However, we can calculate it for one part of data and then go through the other part of data. Therefore, it is necessary to mention what the "read" process is. This process is divided into three steps as may be seen by referring to the flow chart shown in Figure 7.

(1) Initial correction: Read first 500 data values and do calculations of

$$R(j) = \sum_{i=1}^{500} x_i x_{i+j-1} ; \text{ where } j \text{ from 1 to 100} ; \quad \text{AVER} = \sum_{i=1}^{500} x_i$$

(see Figure 7, blocks 12, 13, 14, 15, 16, 17, and 18)

(2) Main loop: Read 1000 data values (i.e. half of the data in first record and half of the data in second record) and do the calculations of

$$R(j) = \sum_{i=1}^{500} x_i x_{i+j-1} ; \text{ where } j \text{ from 1 to 100} ; \quad \text{AVER} = \sum_{i=1}^{500} x_i$$

(see Figure 7, blocks 19, 20, 21, 22, 23, 24, 25, 26, 27, 28, 29) In order to keep reading the data under this form the "read" and "go to" statements have been used to read the data from 501 to $10^5 - 500$. (see Figure 7, blocks 19 and 31)

(3) Final correction. Read the last 500 data values of the last record (i.e. 100th record) and do the following calculations

$$R(j) = \sum_{i=1}^{500} x_i x_{i+j-1} ; \text{ where } j \text{ from 1 to 100} ; \quad \text{AVER} = \sum_{i=1}^{500} x_i ; \quad \bar{x} = \frac{1}{10} \text{AVER}$$

(see Figure 7, blocks 32, 33, 34, 35, 36, 37, 38, 39, 40, and 41)

The calculation of the power spectral density has been divided into two parts. First, calculate the raw power spectral density by equation (25) (see Figure 7, block 63). Second, calculate the smoothed power spectral density by equation (26) (see Figure 7, blocks 66, 67, and 68).

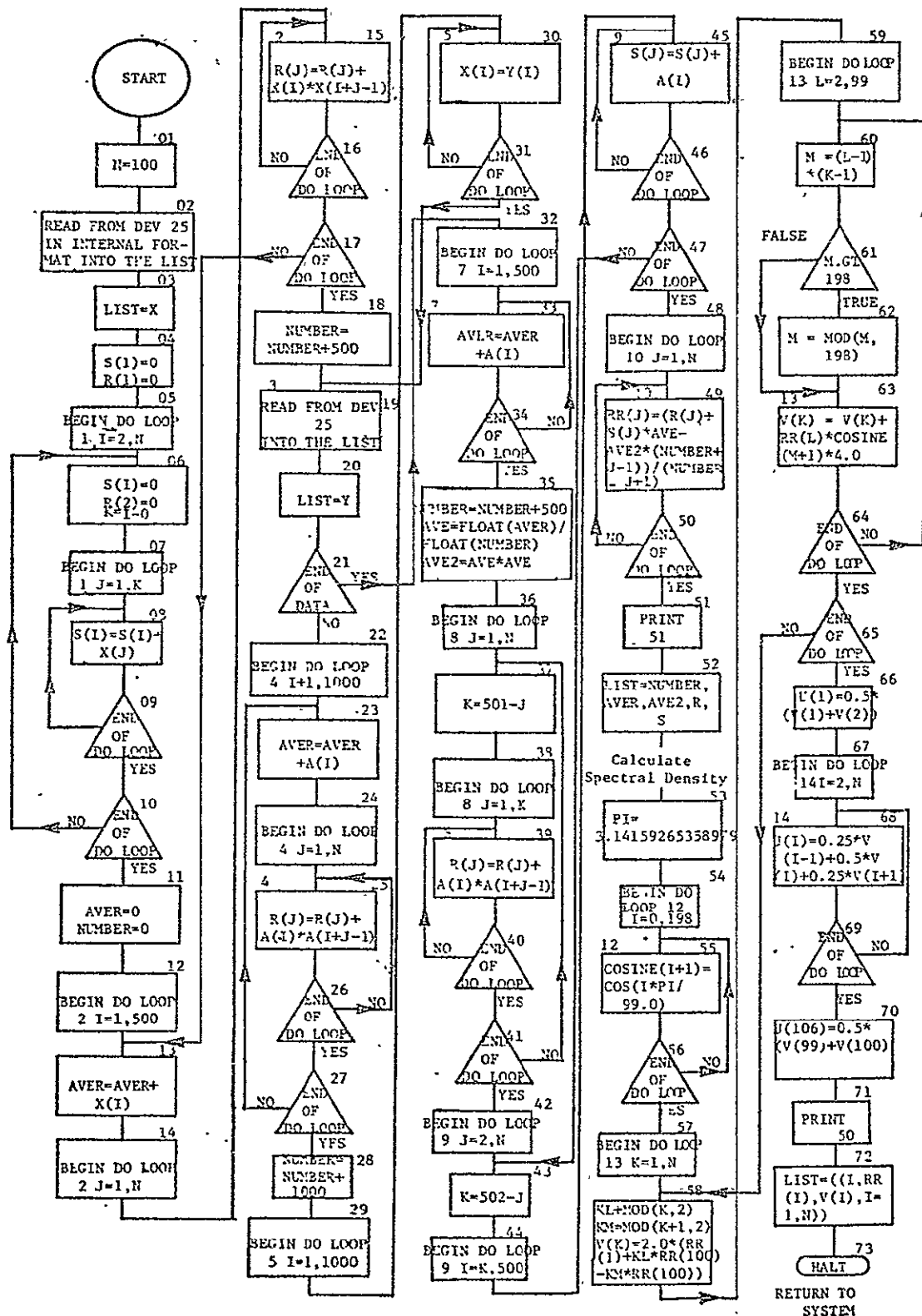


FIGURE 7
Flow Chart of Autocorrelation Function and Power Spectrum

CHAPTER IV

EXAMPLE OF SIMULATED DATA

For the purpose of checking the computer result for the autocorrelation function and power spectrum for the simulated data generated by computer, the analytical solution for the autocorrelation function and power spectrum has to be discussed. From the analytical point of view, we use the average value of the simulated data.

4.1 Autocorrelation and Power Spectrum for a Random Background

From KORN (1966a) and BENDAT and PIERSOL (1966d), we know that the random data are not correlated among themselves. However, there is a correlation among individual terms. For example, $x(t_1)$, $x(t_1 + \tau)$ are uncorrelated for every $\Delta t \neq 0$, therefore, autocorrelation function will be a delta function at lag time zero, i.e. $\tau = 0$ for infinite length of record. The power spectrum would be a constant over all the frequency range. This is so called white noise. In other words, white noise has a constant power spectral density, i.e. $G(f) = a$, $R(\tau) = a\delta(\tau)$ where a is constant. Unfortunately, such a process for white noise is not physically realizable since the variance or $R(0)$ is infinite. This is true for only infinite length of record.

In practice, white noise is approximated by various types of wide-band noise, having approximately constant spectral density over a frequency band of interest ("band-limited white noise"). From BENDAT and PIERSOL (1966e), bandwidth limited white noise is a random process with a constant

power spectrum defined by

$$\begin{aligned} G(f) &= a & 0 \leq f_0 - (B/2) \leq f \leq f_0 + (B/2) \\ &= 0 & \text{otherwise} \end{aligned} \quad (27)$$

where f_0 is the center frequency, and B is the bandwidth. From equation

(15) it follows that the associated autocorrelation function is

$$R(\tau) = \int_{f_0 - (B/2)}^{f_0 + (B/2)} a \cos 2\pi f \, df = aB \left(\frac{\sin \pi B \tau}{\pi B \tau} \right) \cos 2\pi f_0 \tau$$

For the low-pass white noise, $f_0 = \frac{B}{2}$, then $G(f)$ becomes

$$G(f) = a \quad 0 \leq f \leq B \quad (28)$$

$$= 0 \quad \text{otherwise}$$

and $R(\tau) = aB \left(\frac{\sin 2\pi B \tau}{2\pi B \tau} \right)$

In Figure 8, the frequency information we want is in the low range of frequencies. So the low-pass white noise is of interest. The autocorrelation function for low-pass white noise is a sinc function which looks like the amplitude of the diffraction pattern for the single slit.

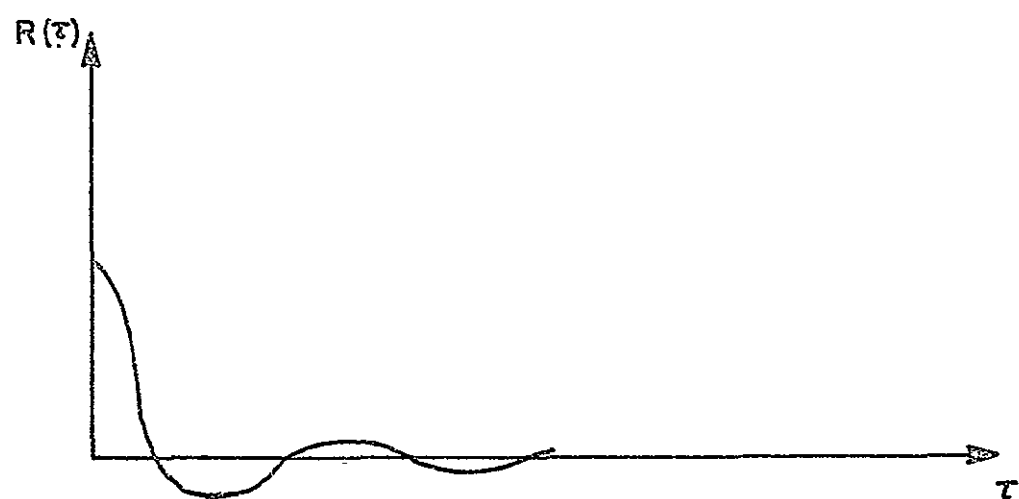
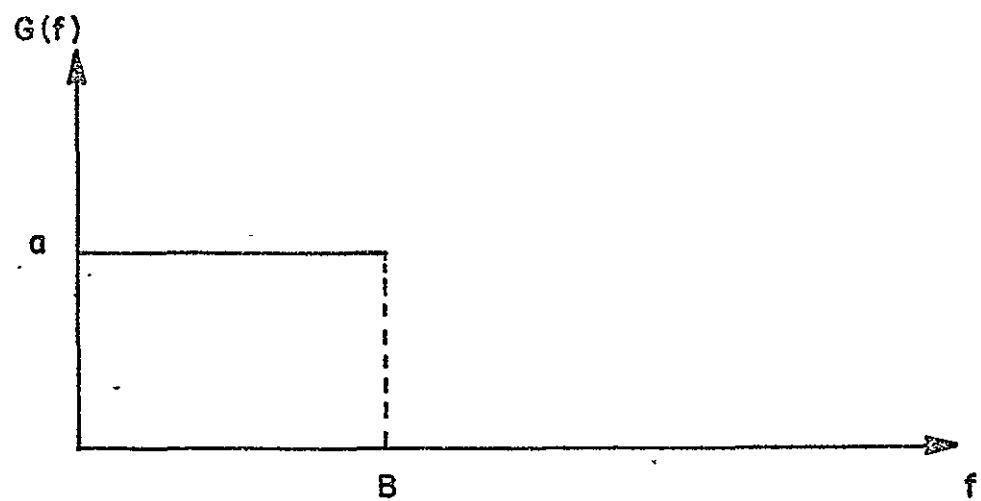


FIGURE 8

4.2 Autocorrelation and Power Spectrum Prediction for the Average Pulse Signal Above an Average Random Background

In this section we discuss a square pulse above the random background with period T . If we make this average square pulse signal with a 100% intensity increase over the background for a time $T/2$ and off for the remaining time $T/2$, then we ask: What will the autocorrelation function and power spectral density function look like?

Before analyzing and making this clear, the Autocorrelation theorem will have to be reexamined.

Autocorrelation Theorem

If $x(t)$ has the Fourier transform $A(f)$, then its autocorrelation function $\int_{-\infty}^{\infty} x^*(t)x(t+\tau)dt$ has the Fourier transform $|A(f)|^2$, i.e.

$$\int_{-\infty}^{\infty} |A(f)|^2 e^{i2\pi f \tau} df = \int_{-\infty}^{\infty} x^*(t)x(t+\tau)dt = R(\tau) \quad (16)$$

This is the unnormalized autocorrelation function with zero mean.

Suppose there is a rectangle function $II(t)$ which is defined such that

$$\begin{aligned} II(t) &= 1 & |t| < \frac{1}{2} \\ &= 0 & |t| > \frac{1}{2} \end{aligned}$$

The Fourier transformation of the function $II(t)$ is $\text{sinc}(f) \equiv \frac{\sin \pi f t}{\pi f t}$

Therefore, using the Autocorrelation theorem, the $R(\tau)$ is the Fourier transform of $\text{sinc}^2 f$ function is the triangle function of unit height and area.

This function $\Lambda(\tau)$ is defined that

$$= 1 - |\tau| \quad |\tau| < 1$$

$$\begin{aligned} \Lambda(\tau) &= 0 & |\tau| > 1 \end{aligned}$$

These transformations are shown by three solid arrows and one dashed arrow in Fig. 9. Any arrow represents a Fourier transformation. The lower solid arrow in Fig. 9 indicates that power spectrum is transformed to the autocorrelation function and the dashed arrow represents the inverse transformation.

From the above transformations we know that a $II(t)$ function for the signal will result in a triangular shaped autocorrelation function. If you concentrate, the positive side of t axis of $II(t)$, you will have a straight line together with two axes which can form 45° right triangle. The autocorrelation function of the average square pulse signal above an average background will be of a triangular shape along the lag time axis.

For the purpose of making the autocorrelation function of the square pulse signal clear, we show a plot of the average square pulse signal above the average background, and its autocorrelation function in Fig. 10. Part (a) of Fig. 10 shows the square pulse signal above an average background. In order to calculate an autocorrelation function for zero mean, we use the data in part (b) of Figure 10 which is made by shifting the mean value of signal and background. Part (c) of Figure 10 represents the autocorrelation function for the case of zero mean. It is seen that the period of the autocorrelation function is the same as that of average signal above the average background.

Mathematically speaking, the autocorrelation function qualitatively can be considered as the product of the same waveform with a lag time τ between each other.

(1) When the lag time τ equals zero, the normalized autocorrelation function must be the maximum value 1 [see Figure 10 (c), a].

(2) When the lag time $\tau = \frac{T}{4}$, where T is the period of signal, the product is zero [see Figure 10 (c), b].

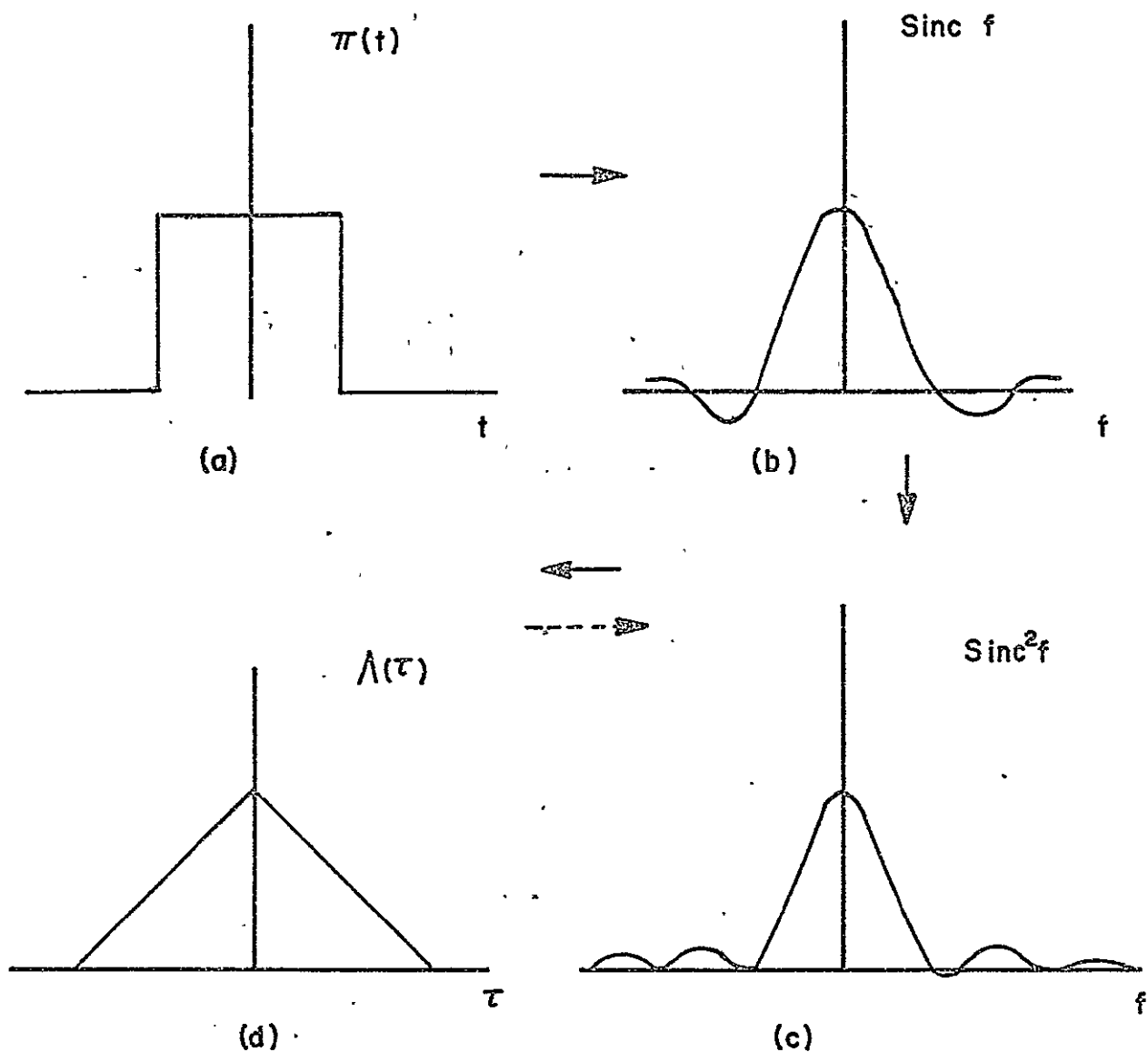


FIGURE 9

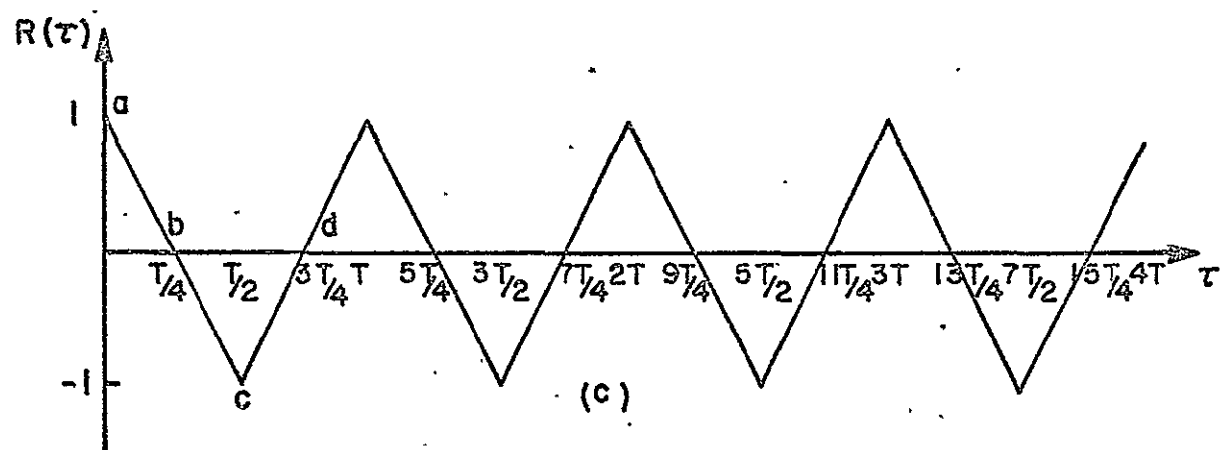
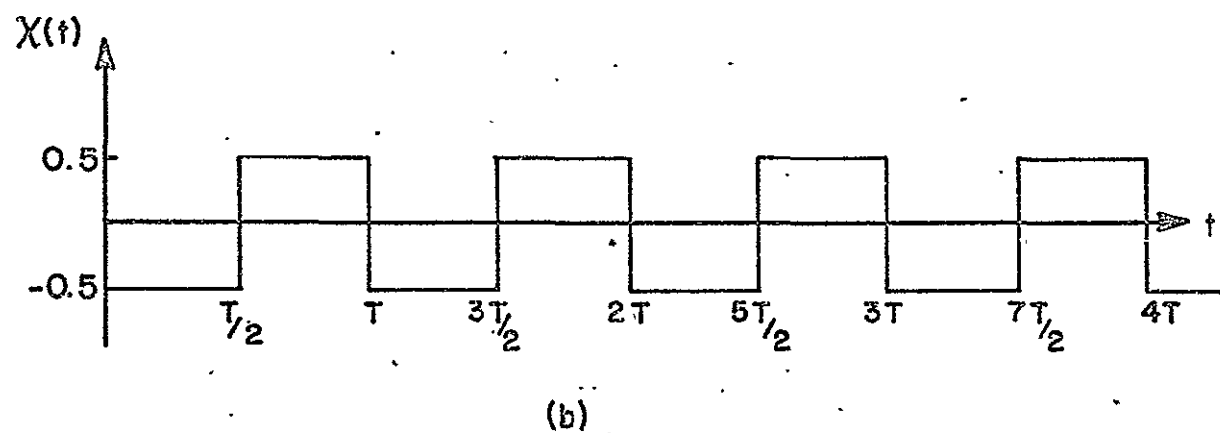
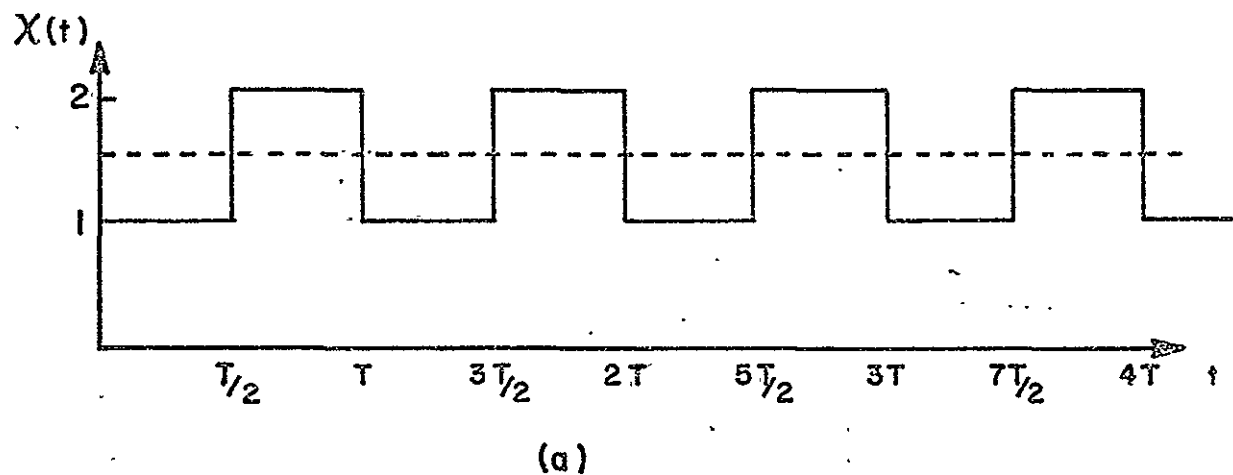


FIGURE 10

(3) When the lag time $\tau = \frac{T}{2}$, i.e., out of phase completely, the product is minimum value = 1 [see Figure 10 (c), c].

Similarly you will have $R(\frac{3T}{4}) = 0$, $R(T) = 1$, etc.

Power Spectrum

There are two ways to calculate the power spectral density function $G(f)$ for the average square pulse above the average background.

(1) The density function $G(f)$ can be considered as the Fourier transform of the autocorrelation function. In other words, the shape of $G(f)$ will be $\text{sinc}^2 f$ function of the positive range when $A(\tau)$ is the autocorrelation function. In this plot there will be several peaks at several particular frequencies but the amplitude of these peaks will be gradually smaller and then die out for increasing frequency f .

(2) Ratio of the power of one component to the other:

From the mathematical derivation equation (13) we have the result $R(0) = \overline{X(t)^2} = \int_0^\infty G(f)df$ where $\overline{X(t)^2}$ is referred to as the time averaged power of the mean power in $X(t)$. Consider

$$X(t) = \frac{a_0}{2} + \sum_{n=1}^{\infty} (a_n \cos 2\pi f_n t + b_n \sin 2\pi f_n t)$$

where $f_n = \frac{n}{T}$, and a_0 , a_n and b_n are the usual Fourier coefficients.

Then by the orthogonality of the sine and cosine functions

$$\overline{X^2(t)} = \lim_{T \rightarrow \infty} \frac{1}{2T} \int_{-T}^T X^2(t) dt = \left(\frac{a_0}{2}\right)^2 + \frac{1}{2} \sum_{n=1}^{\infty} (a_n^2 + b_n^2) = C_0^2 + \frac{1}{2} \sum_{n=1}^{\infty} C_n^2$$

$$\text{Where } C_0 = \frac{a_0^2}{2}, \quad C_n = (a_n^2 + b_n^2)^{\frac{1}{2}}$$

The amplitude, C_n of a certain frequency, f_n can be found out by taking the area under the peak above the average noise level and equating it to $\frac{1}{2}C_n^2$.

Theoretically, in the case of a square wave $X(t) = \frac{2}{\pi} \sum_{n=1,3,\dots} \frac{1}{n} \sin\left(\frac{2n\pi t}{T}\right)$ the ratio of the power of the fundamental component to that of first harmonic component is

$$\frac{1}{2} C_1^2 : \frac{1}{2} C_3^2 = C_1^2 : C_3^2 = \left(\frac{2}{\pi}\right)^2 : \left(\frac{2}{\pi}\right)^2 \left(\frac{1}{3}\right)^2 = 9 : 1$$

Similarly $C_1^2 : C_5^2 = 25 : 1$ etc.

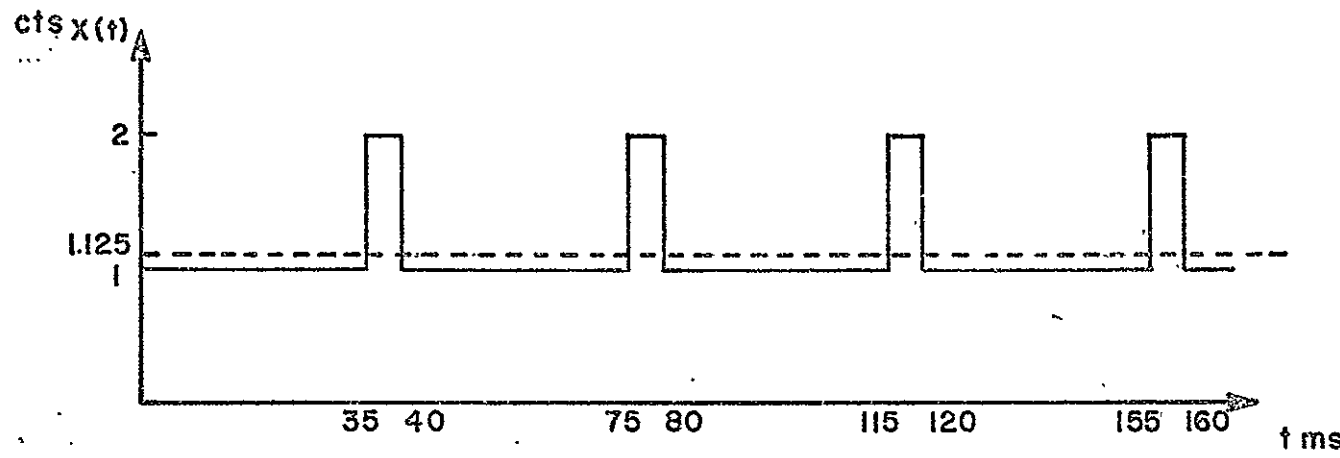
4.3 Autocorrelation and Power Spectrum Prediction for the Average Pulsar Signal Above an Average Random Background

The pulsar type signal used is a pulse which is off 35 ms with an average counting rate 1 count/ms and on 5 ms with an average counting rate 2 count/ms. In order to calculate the autocorrelation function with zero mean, we have to transform from this [Figure 11 (a)] to the one which forms the autocorrelation function with zero mean as shown in (b) of Figure 11. Figure 11 (c) indicates the corresponding autocorrelation function for the case of (b).

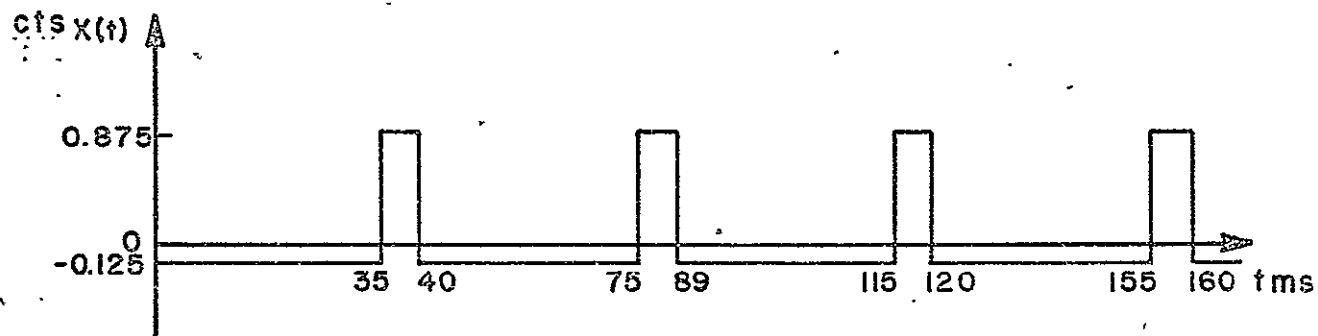
For the same reason as discussed for the autocorrelation of an average square pulse signal the shape of the autocorrelation function is triangular. KORN (1966b) shows that the minimum value is a negative number $-\sigma^2/N = -1/8$ where σ^2 is the variance which is equivalent to autocorrelation function at zero lag time, and N is the period divided by the on time. For the case (b) Figure 11, the triangle has a base of 10 ms. The period of autocorrelation is 40 ms which is same as the signal [Figure 11 (c)]. When the lag time is 40 ms, i.e., the period, the two identical waveforms are superimposed completely; i.e., the product of two identical data is maximum and this is the case whenever the lag time is a multiple number of periods. It is a constant negative number $-1/8$ for the rest of ranges except when τ is in the range of 0~5 ms, 35~45 ms, 75~85 ms, etc.

The simulated data $X(t)$ in Figure 11 (b) has a Fourier series of the form:

$$X(t) = \frac{a_0}{2} + \sum_{n=1}^{\infty} a_n \sin\left(\frac{2n\pi t}{T}\right) + \sum_{n=1}^{\infty} b_n \cos\left(\frac{2n\pi t}{T}\right)$$



(a)



(b)

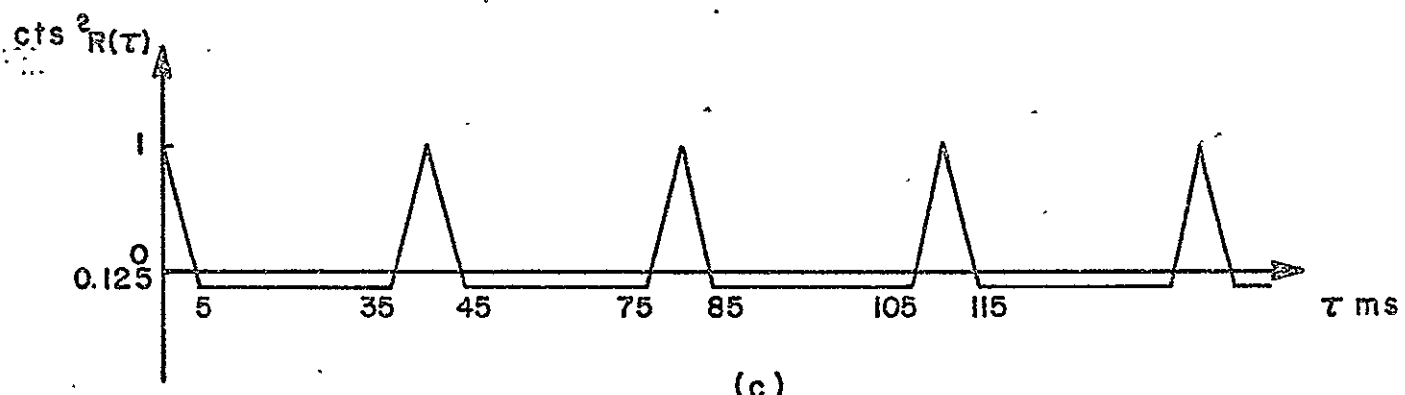


FIGURE 11

where

$$\begin{aligned} x(t) &= -0.125 & 0 < t < \frac{7}{8}T \\ &= 0.875 & \frac{7T}{8} < t < T \end{aligned}$$

$$a_0 = \frac{2}{T} \int_0^T x(t) dt = 0$$

$$a_n = \frac{2}{T} \int_0^T x(t) \sin\left(\frac{2n\pi t}{T}\right) dt = \frac{1}{n\pi} \left[\cos\left(\frac{7n\pi}{4}\right) - 1 \right]$$

$$b_n = \frac{2}{T} \int_0^T x(t) \cos\left(\frac{2n\pi t}{T}\right) dt = -\frac{1}{n\pi} \sin\left(\frac{7n\pi}{4}\right)$$

$$\begin{aligned} c_n^2 &= a_n^2 + b_n^2 \\ &= \left(\frac{1}{n\pi}\right)^2 \left\{ \left[\cos\left(\frac{7n\pi}{4}\right) - 1 \right]^2 + \sin^2\left(\frac{7n\pi}{4}\right) \right\} \\ &= \frac{2}{n^2\pi^2} \left[1 - \cos\left(\frac{7\pi n}{4}\right) \right] \end{aligned}$$

Therefore, the ratio of the power in the fundamental frequency to that of third harmonic frequency is

$$\frac{c_1^2}{c_3^2} = \frac{\frac{2}{\pi^2} \times 0.298}{\frac{2}{\pi^2} \times 0.19} = \frac{1.57}{1}$$

similarly

$$\frac{c_2^2}{c_4^2} = \frac{\frac{1}{2\pi^2}}{\frac{1}{4\pi^2}} = \frac{2}{1}$$

Using the above result, we can compare the power spectrum calculated by the program with the simulated average pulsar signal above an average random background.

4.4 Computer Results for the Autocorrelation Function and the Power Spectrum With Several Kinds of Simulated Data

The analytical solutions have been examined in the last three sections of this chapter. In this section, I am going to discuss the autocorrelation function and power spectrum for the practical data generated by the computer.

(1) Random Noise

As I mentioned in Section 4.1, $R(\tau)$ would be infinite at the origin and zero throughout all the range of lag time τ in the plot $R(\tau)$ vs τ , and $G(f)$ would be constant throughout all the range of frequency f . In other words, the autocorrelation function is simply a delta function and the constant power spectrum is the so-called white noise.

Practically, all we can have is a definite length of random data. Therefore, from equation (28) the autocorrelation function would be an extremely large value at the origin, but fluctuates with a small deviation about zero throughout the whole range of lag time. [see Figure 12 (a)] The power spectrum also will fluctuate with a small deviation about a constant mean value throughout the range of low frequency we are interested in. This is called low-pass white noise. [see Figure 13 (a)]

The results of $R(\tau)$ and $G(f)$ for the simulated random data are shown in the Figure 12 (a) and Figure 13 (a) respectively. Note the simulated random data has been generated for the average counting rate, 1 count/ms. The sample time was 1 ms, and there were 10^5 data points for total record length of 100 sec.

(2) Square Pulse Signal Above a Random Background

The simulated square pulse signal above the random background fluctuates about the average square pulse above the average random background. In other words, simulated data generated by the computer fluctuates about the average value which was used in the theoretical analysis in Sections 4.1, 4.2, and 4.3. For this reason the autocorrelation function at zero lag time has an extremely large value which is much larger than that expected initially as shown in Figure 11 (c).

The data I used is for an average background rate 1 count/ ms for 20 ms and an increased average rate to 2 counts/ms for 20 ms. In other words, this is the pulse 20 ms off and 20 ms on with 100% intensity above the random background. In order to calculate the autocorrelation function with the zero mean, the mean value has to be subtracted from each datum. This square wave would have 1 unit amplitude difference between maximum and minimum.

As shown in Section 4.2, the autocorrelation function for this kind of data gives a result that is almost the same as shown in Figure 10 (c) except at zero lag time. The shape of $R(\tau)$ is periodic triangular type with a period 40 ms which is the same as the period of the square wave. [see Figure 12 (b)]

The power spectrum $G(f)$ of the average square wave data has the largest high peak at the fundamental frequency (25 cycles/sec) and a second peak at the first harmonic frequency (75 cycles/sec) and a third peak at 125 cycles/sec, etc. The shape of $G(f)$ is approximately $\text{sinc}^2 f$ function as shown in Figure 13 (b).

The power ratio of the fundamental component to the first harmonic component is 9/1 and that of the fundamental component to the second harmonic

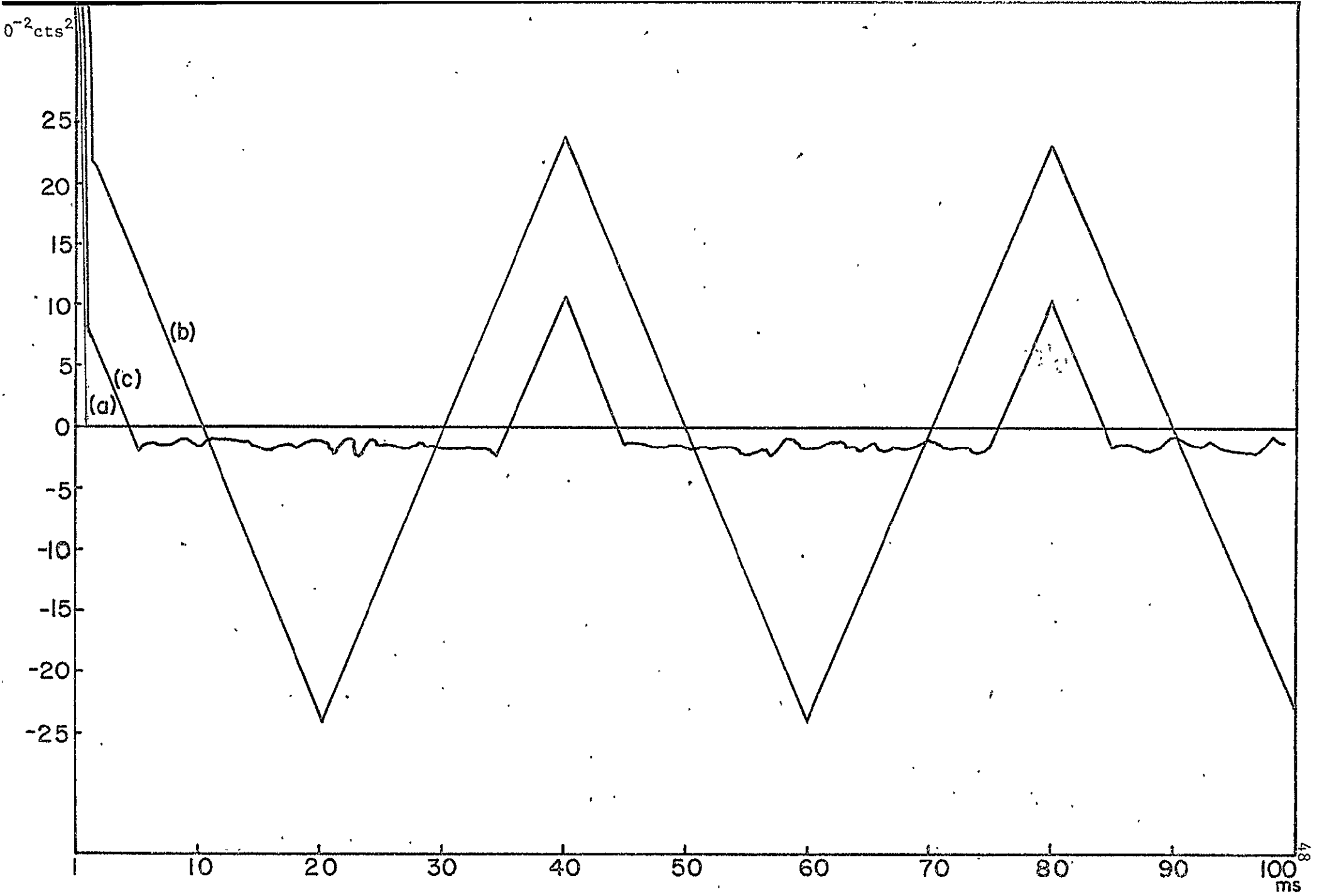
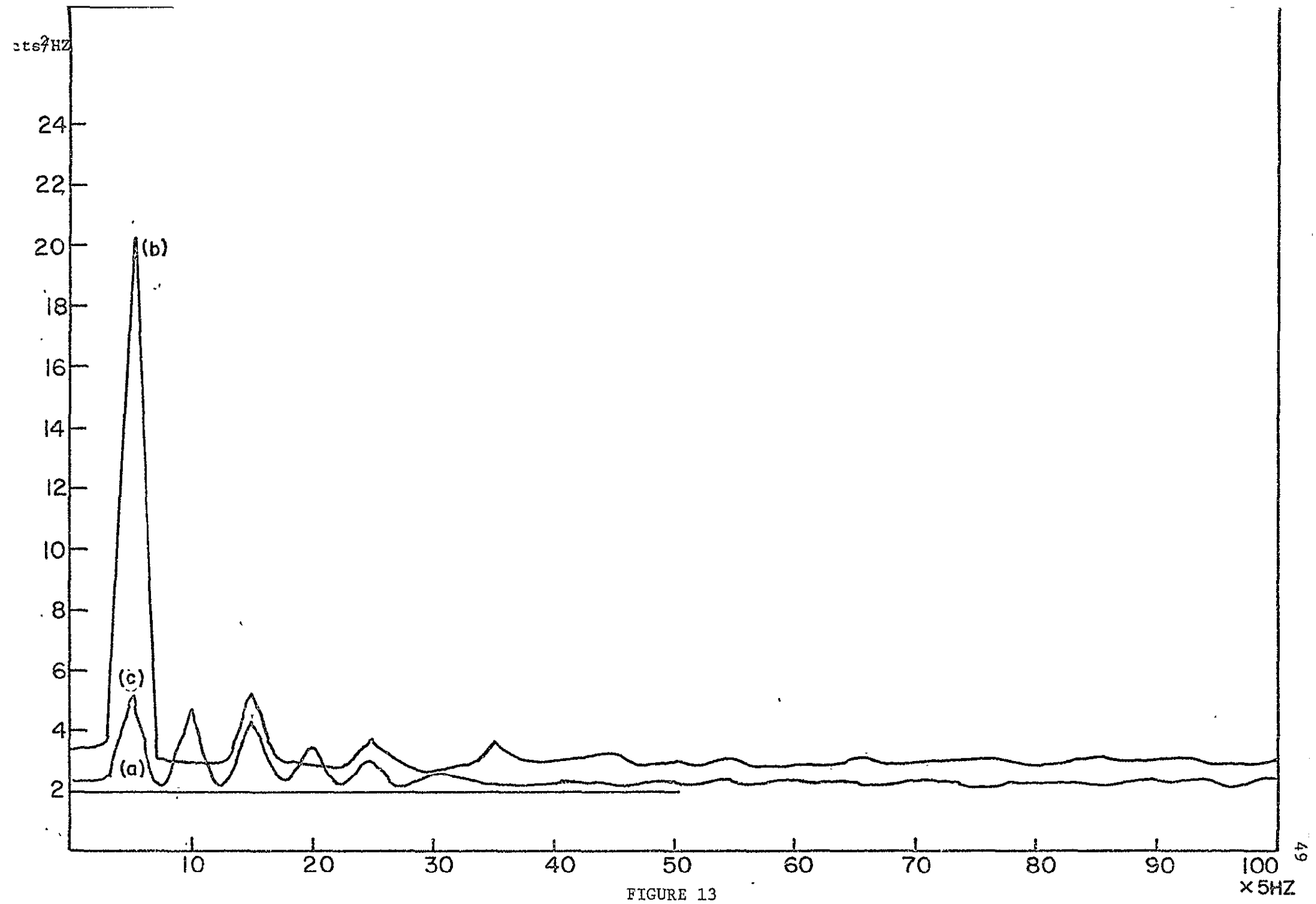


FIGURE 12



ic component is 25/1 theoretically. From the plot of $G(f)$ vs f (Figure 13), and Table 3, we calculate the background of $G(f)$ is 3.008 (counts²/HZ). The computer results gives the power ratios $8.558/1$ and $25.349/1$ with the deviations from the theoretical value of 4.9% and 1.4% respectively. However, the value of $G(f)$ beyond the third peak at 175 cycles/sec is not so good compared with the theoretical value. The method of calculation of the power ratios is shown in the Appendix D.

(3) Pulsar Type Signal Above a Random Background

These simulated data are the same as for the case of the square pulse above a random background data except that the pulse type signal is off 35 ms and on for 5 ms.

Like the case of the square pulse signal above random background, the autocorrelation function has an extremely large value at zero lag time. This value is different from the one at larger lag times. This extremely large value is about ten times larger than the other peak values, because two identical fluctuating pulsar waveforms are completely in phase at the zero lag time. In the Figure 12 (c), there are two triangles with peaks at 40 ms and 80 ms, respectively. The base of the triangle is 10 ms.

The calculation of power spectrum can be checked by the power ratio method. The power spectrum $G(f)$ of the pulsar type signal above random background has the largest peak at the fundamental frequency (25cycle/sec) and a second peak at the first harmonic frequency (50 cycle/sec) and a third at 75 cycle/sec. [see Figure 13 (c)]

Theoretically, the power ratio of the fundamental component to the second harmonic component is $1.57/1$, and that of the first harmonic component to the third harmonic component is $2/1$. From Figure 13 and Table 4, the power spectrum of the random background of $G(f)$ is 2.248 (counts²/HZ).

TABLE 3

1	1.74254513	3.40725613
2	0.21791589	3.55436420
3	0.20155525	3.53161335
4	0.17607462	3.62998962
5	0.15360302	13.33540595
6	0.13336164	21.92366943
7	0.10707951	11.80975492
8	0.06996548	2.99213219
9	0.04641684	3.11158371
10	0.03575322	3.05784705
11	0.00867837	3.02836581
12	-0.01015049	2.90592085
13	-0.04252198	2.85753155
14	-0.06766814	3.04165459
15	-0.09294486	4.44231701
16	-0.11213052	5.22297573
17	-0.13548291	3.72302216
18	-0.15690041	2.83215923
19	-0.18556464	3.01939774
20	-0.21144891	3.04004669
21	-0.24250412	2.94048214
22	-0.21030223	2.90934535
23	-0.13263578	2.90762615
24	-0.15310770	2.93473625
25	-0.13339764	3.46660805
26	-0.12215799	3.75395321
27	-0.09528977	3.28968620
28	-0.06813085	2.92237759
29	-0.04189673	2.71464672
30	-0.01995829	2.74388039
31	-0.00061018	2.739885006
32	0.02220001	2.86302090
33	0.04318444	2.95668205
34	0.07140726	2.96916771
35	0.08506513	3.43024731
36	0.10841668	3.65500950
37	0.13342428	3.52032967
38	0.15617090	3.07000446
39	0.18409115	3.00108242
40	0.21716279	2.95348353
41	0.23207843	2.99359142
42	0.20889372	3.08365154
43	0.18459249	3.09661770
44	0.16136748	3.11090660
45	0.14315361	3.29538727
46	0.11523497	3.25720119
47	0.09401387	2.99019814
48	0.06061661	2.92143631
49	0.03843407	2.90792942
50	0.01875231	2.92412949

/ NOT REPRODUCIBLE /

51	-0.00931841	2.99452696
52	-0.02269282	2.95785427
53	-0.04548740	2.91138458
54	-0.06685668	2.98374950
55	-0.09799665	3.11750989
56	-0.10921627	3.07626057
57	-0.14244288	2.96743298
58	-0.15874672	2.96641445
59	-0.19177997	2.92331028
60	-0.20400161	2.92315669
61	-0.24262869	3.01554394
62	-0.20773232	3.03054810
63	-0.18753499	2.97146893
64	-0.15474308	2.97667408
65	-0.14004272	3.129446701
66	-0.12049399	3.19570923
67	-0.09132838	3.10769272
68	-0.06784606	3.06819153
69	-0.04742037	3.05442333
70	-0.02699487	3.02104282
71	-0.00150418	2.99955273
72	0.01964332	3.03165531
73	0.04824098	3.06587410
74	0.06390601	3.08440113
75	0.09397078	3.12718868
76	0.11043715	3.08937263
77	0.14000326	3.02504063
78	0.15429318	3.04276943
79	0.17974269	2.98475075
80	0.21000022	2.88011456
81	0.23227769	2.91168880
82	0.20423537	2.98068714
83	0.18657492	3.00754261
84	0.16334558	3.05957054
85	0.14215624	3.14396381
86	0.11398625	3.10764503
87	0.08794248	3.03852654
88	0.05977638	3.01292229
89	0.03124937	2.96162510
90	0.02007224	2.98826694
91	-0.00808540	3.12558355
92	-0.02097471	3.13164616
93	-0.04971886	2.99409485
94	-0.06927502	3.10826111
95	-0.09534270	3.23718643
96	-0.11247742	3.05253220
97	-0.14215893	2.99043751
98	-0.15275878	3.05138588
99	-0.18744117	2.94681549
100	-0.20957309	2.85121822

TABLE 4

1	1.23077583	2.24219894
2	0.08200514	2.24840641
3	0.05716614	2.27999592
4	0.03336975	2.31953049
5	0.01275801	3.80827808
6	-0.01928971	5.12577915
7	-0.01361207	3.55628395
8	-0.01756435	2.16644764
9	-0.01518434	2.28440285
10	-0.00984651	3.67682838
11	-0.01661853	4.66694482
12	-0.01158940	3.20044231
13	-0.01269277	2.12567234
14	-0.01237036	2.30790234
15	-0.01249175	3.40310764
16	-0.01921413	4.15856171
17	-0.01986755	3.08336353
18	-0.01389924	2.24613667
19	-0.01839143	2.30779648
20	-0.01372823	3.10451031
21	-0.01183049	3.56556892
22	-0.02295482	2.71351814
23	-0.01185386	2.17718506
24	-0.01904688	2.27599621
25	-0.01006116	2.68459225
26	-0.01475369	2.91632175
27	-0.01448439	2.48085117
28	-0.01738782	2.15563011
29	-0.01266667	2.17639446
30	-0.01702931	2.39418888
31	-0.01823109	2.58086681
32	-0.01640008	2.43372345
33	-0.01339928	2.26201916
34	-0.01488116	2.25613213
35	-0.01738278	2.27603912
36	-0.02859438	2.25998020
37	0.01446395	2.22689152
38	0.02969724	2.22111607
39	0.06513095	2.21027374
40	0.08022875	2.18391705
41	0.10867971	2.20649910
42	0.08430517	2.26772690
43	0.05794246	2.30425739
44	0.02888179	2.35013866
45	0.00863192	2.36390305
46	-0.01216547	2.25334454
47	-0.01331612	2.17950630
48	-0.01524717	2.26031399
49	-0.01596766	2.38119507
50	-0.01313644	2.42072296

NOT REPRODUCIBLE

51	-0.01592108	2.35191727
52	-0.01482943	2.24920177
53	-0.01630285	2.20243549
54	-0.01557263	2.27754116
55	-0.01576539	2.41936684
56	-0.02212092	2.37709427
57	-0.01728968	2.25894451
58	-0.02213512	2.26483631
59	-0.01148916	2.30453110
60	-0.01676009	2.41067028
61	-0.01603152	2.42852116
62	-0.01574961	2.32445049
63	-0.01091176	2.25980949
64	-0.01216391	2.29706669
65	-0.01890835	2.38499451
66	-0.01276767	2.33801842
67	-0.01801877	2.25986481
68	-0.01522582	2.25233269
69	-0.01611783	2.26955414
70	-0.01601792	2.31738949
71	-0.01016211	2.38268757
72	-0.01476673	2.38652134
73	-0.01473686	2.32282066
74	-0.01387888	2.28016090
75	-0.02071720	2.25579624
76	-0.01343445	2.12461281
77	0.01087264	2.14761925
78	0.03875672	2.18167877
79	0.06787103	2.17203236
80	0.08175081	2.15672398
81	0.10591346	2.14904022
82	0.07978457	2.23986244
83	0.05971146	2.32242298
84	0.03181953	2.28068924
85	0.01426323	2.24168110
86	-0.01540809	2.18393517
87	-0.01236438	2.11809349
88	-0.01426741	2.18995857
89	-0.01941834	2.35678959
90	-0.01624508	2.42445564
91	-0.00618494	2.31532288
92	-0.01317261	2.26659775
93	-0.01684612	2.32386780
94	-0.01159265	2.37490463
95	-0.01721993	2.39006996
96	-0.01708999	2.25011826
97	-0.02087504	2.13265610
98	-0.02069632	2.19956779
99	-0.00612100	2.41071129
100	-0.01110787	2.55776882

NOT REPRODUCIBLE

The computer results for the power ratio are 1.47/1 for the fundamental component to the second harmonic component, and 1.81/1 for the first harmonic component to the third harmonic component. The deviations from the theoretical average are 6% for the former case and 9.5% for the latter case.

(4) Smallest Detectable Pulsar Using Autocorrelation and Power Spectrum Analysis

The autocorrelation and power spectrum measurements for the pulsar signal with 100% intensity above the random background have been shown in section 4.4.3, the result of this analysis shows that the autocorrelation function and power spectrum are detectable and predictable.

If we reduce the intensity of signal, can we still detect the autocorrelation function and power spectrum? What is the smallest detectable pulsar signal above the random background? Experimentally, for the pulsar signal with 25% intensity with respect to the random background, the autocorrelation function is not detectable. It is more or less random. (see Figure 14) But the power spectrum in the frequency domain is detectable. If you plot power spectrum versus frequency in a large scale, you still can see the several peaks at the several expected frequencies (see Figure 15). Of course, this curve is not as good as for the case with 100% intensity pulsar signal. The values of the power spectrum over all the frequency range are not fluctuating very much. It can be imagined that the measurement of autocorrelation function and power spectrum will be getting worse and worse for reducing the intensity of pulsar signal smaller and smaller. If you keep reducing the intensity of signal, finally the result will turn out to be the case of random background. Then the autocorrelation function and power spec-

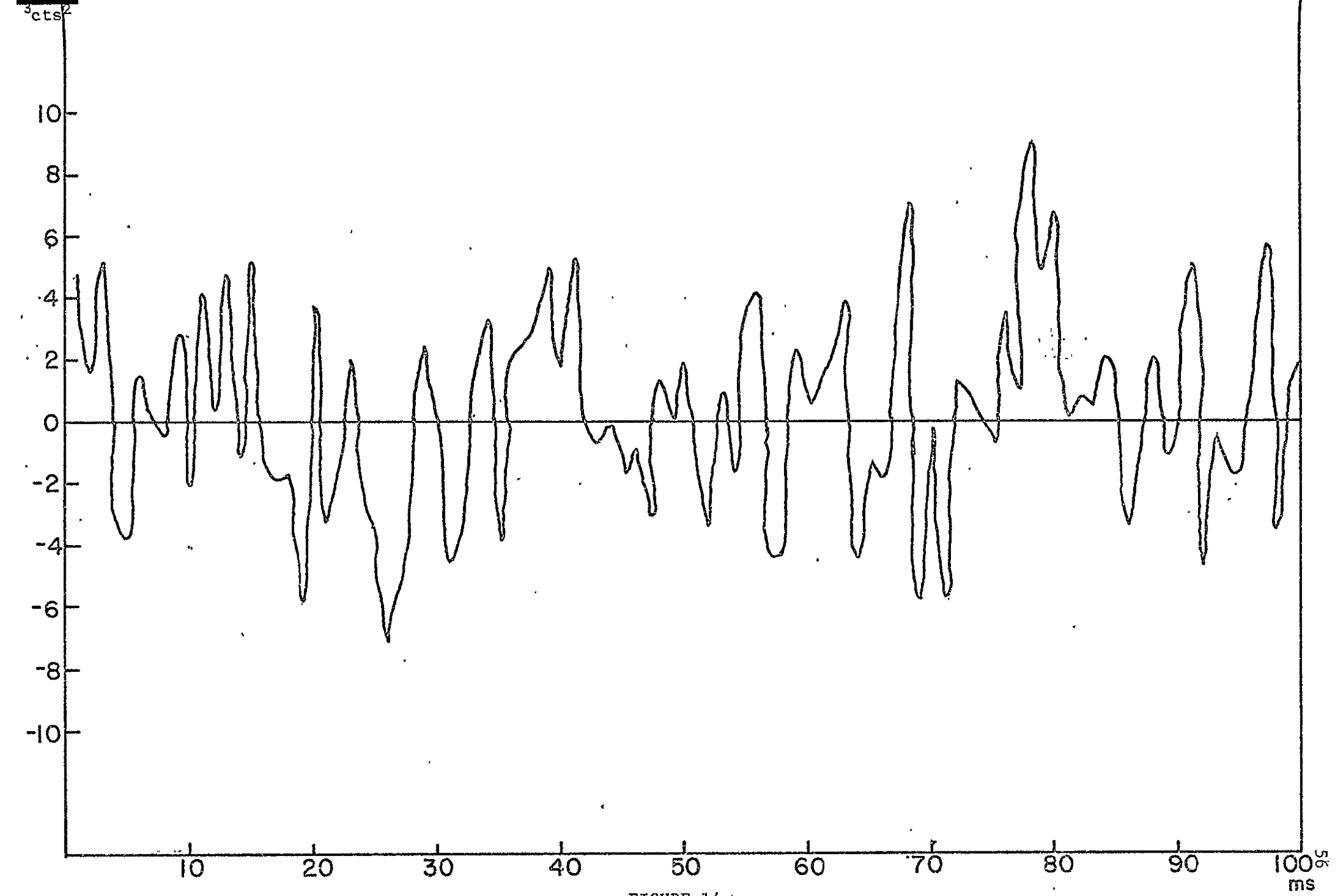
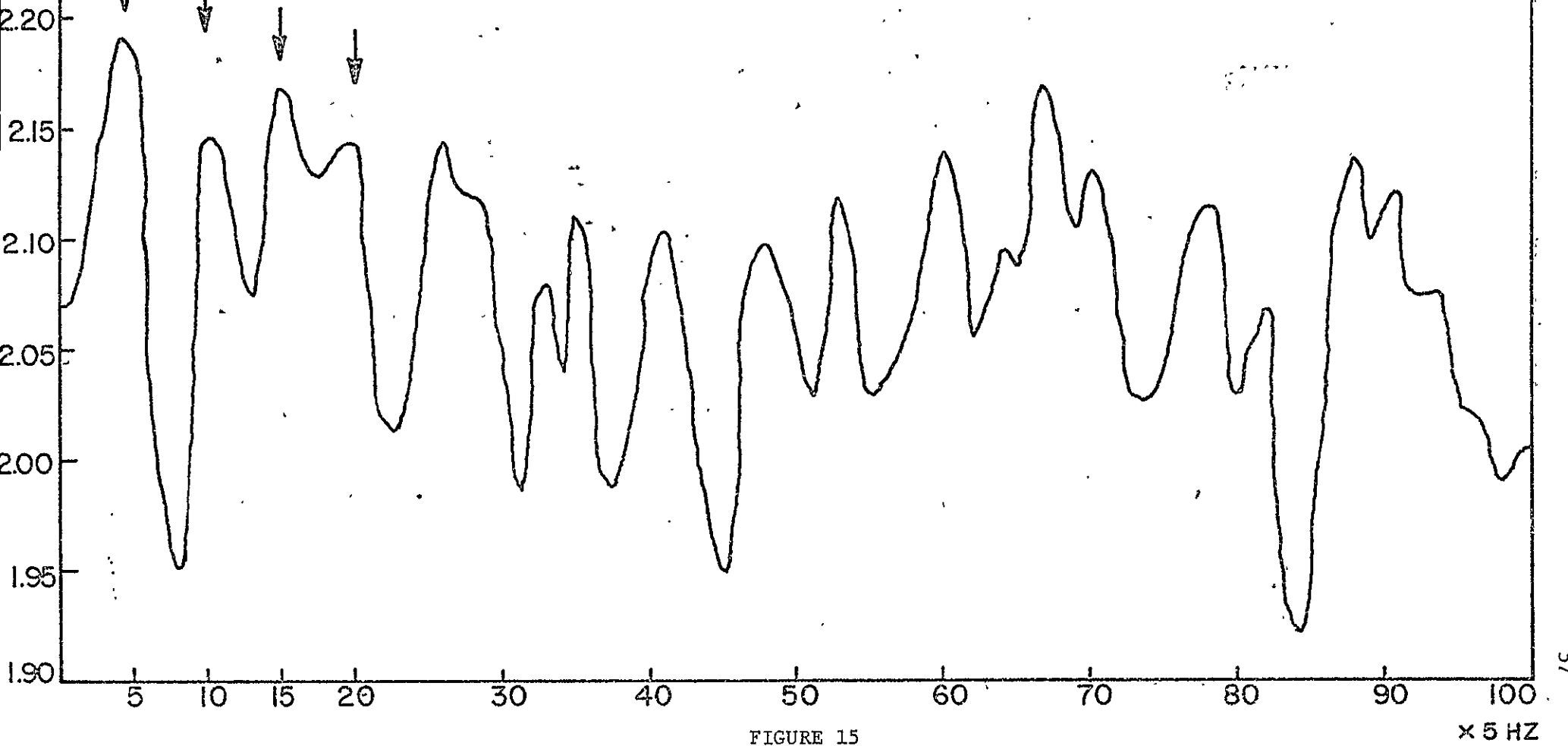


FIGURE 14



trum would be sinc function and approximately a constant with small deviation, respectively. This result is based upon the short data record of length 100 sec and the sampling time of 1 ms.

It is interesting that a pulsar with 0.5% intensity above random background can be detected by use of superimposed Epoch Analysis as done by LARRY ORWIG for NP 0532, (1971).

CHAPTER V

CONCLUSION AND DISCUSSION

Autocorrelation and power spectrum technique detects periodic signals from the random noise. However, the power spectrum also determines the power of each frequency component. For the actual X-ray or gamma ray pulsar NP 0532, this method reveals the power of the pulsating component. Of course, the power of pulsating component of NP 0532 depends on the photon energy range you are interested in.

The simulated pulsar data for the autocorrelation and power spectrum analysis are done for the situation of the pulsar signal with 100% intensity above the random background. For this data, the result of autocorrelation and power spectrum shows the pulsating period or pulsating frequency component explicitly.

Reducing the intensity of the signal, the result of autocorrelation and power spectrum analysis is not as good as for the case of a 100% intensity of pulsar signal. The author has done the case of a 25% intensity of signal. The result has been shown in Section 4.4.4. The problem arises from shrinking the intensity of signal above the random noise. The reason is that the fluctuation of the random background is so large that it buries the small intensity signal. We define the fluctuation of the random background as the noise. Therefore, how to reduce the noise (fluctuation) is our main task. There is one way that can be used to solve this problem. That is to increase the number of data points or observation time. The distribution of the number of counts within a unit time interval obeys the Poisson distribution. Therefore, the standard deviation σ equals square

root of the mean value of counts.

For a given average counting rate, δ is proportional to square root of observation time. However, the signal is proportional to the observation time. Then the signal to noise ratio must increase some factor because of increasing the observation time. For example, suppose the signal with 25% intensity on the random background with average counting rate \bar{a} and the observation time t , then the signal to noise ratio is $\frac{S}{\eta} = \frac{0.25 \bar{a} t}{\sqrt{\bar{a} t}} = 0.25 \sqrt{\bar{a} t}$. In the long run, the signal to noise ratio is proportional to the square root of observation time for a given average counting rate \bar{a} .

The power spectral density calculated could be increased if we restrict the analysis to only the frequency range of interest for the simulated pulsar in the original data or if we restrict the power spectrum analysis to only the lowest frequency components of interest. The total power contributed by these low frequency components is equal to the area bounded by the relevant portion of curve of the spectrum and the estimated mean level of the background. The area can be calculated by summing up the spectrum multiplied by the frequency resolution for the discrete case i.e. $P = \sum f_x(f) \Delta f_x$. We could reduce the frequency resolution to get a higher value of the power spectral density for the frequency of interest. The frequency resolution can be expressed as follows:

$$\Delta f = \frac{1}{2m \Delta t}$$

Where m is the maximum lag number and Δt is the sampling time interval.

In other words, the frequency resolution can be reduced by increasing the sample time interval for a given m .

Take the case which I have used for an example. A small signal above the random background would be able to be detected by increasing the sampling time to five times longer than used in the original analysis.

That is, if the sampling time is 5 ms rather than 1 ms the peak in the power spectral density plot would just be discernible. For the shorter sampling time a 25% signal is just discernible. With a 5 ms sampling time a signal of magnitude $25\%/\sqrt{5} \sim 11\%$ would be discernible because the power is proportional to the square of the amplitude.

REFERENCES

BARTLETT, M.S.: 1950, Biometrika., 37, 1.

BENDAT, J.S.: 1958, Principles and Applications of Random Noise Theory, 44, John Wiley & Sons, Inc., New York.

BENDAT, J.S., and PIERSOL, A.G.: 1966(a), Measurement and Analysis of Random Data, 292, John Wiley & Sons, Inc., New York.

Ibid., (b), 279.

Ibid., (c), 280.

Ibid., (d), 87.

Ibid., (e), 85.

BLACKMAN, R.B., and TUKEY, J.W.: 1958(a), The Measurement of Power Spectra, 121, Dover Publications, Inc., New York.

Ibid., (b), 95.

Ibid., (c), 31.

Ibid., (d), 32.

BRACEWELL, R: 1965, The Fourier Transform and Its Applications, 115, McGraw-Hill Book Company, New York.

COCKE, W.J., DISNEY, M.J., and TAYLOR, D.J.: 1969, Nature 221, 525.

EVANS, R.D.: 1955, The Atomic Nucleus, 753, McGraw-Hill Book Company, New York.

FRIEDMAN, H., CHUBB, T.A., MEEKINS, J.F., HENRY, R.C. and FRITZ, G.: 1969, Science 164, 709.

HEWISH, A., BELL, S.J., PILKINGTON, J.D.H., SCOTT, P.F., and COLLINS, R.A.: 1968, Nature 217, 709.

KHARKEVICH, A.A: 1960(a), Spectra and Analysis, 14, Consultants Bureau,
New York.

Ibid., (b), 77.

KORN, G.A.: 1966(a), Randon-Process Simulation and Measurements, 9,
McGraw-Hill Book Company, New York.

Ibid., (b), 86.

ORWIG. L.E., CHUPP, E.L. and FORREST, D.J.: 1971, Nature 231, 171.

STAELIN, D.H., and REIFENSTEIN, E.C.: 1968, Science 162, 1481.

APPENDIX A

FLOW CHART FOR GENERATING SIMULATED RANDOM DATA

A subroutine RANDU was used to generate the random data, corresponding to some average rate \bar{a} . The basic principle and the procedure of generating random numbers within each specified time interval Δt is discussed in section 3.1. From systems/360 scientific subroutine package, this subroutine is expressed by RANDU (IX, IY, UNIT). IX is the first entry; this must be any odd integer number with nine or less digits. After IX entry, IX should be the previous value of IY computed by this subroutine. IY is a resultant integral random number required for the next entry to this subroutine. The range of this number is between 0 and 2^{31} . UNIT is the resultant uniformly distributed, floating point, random number in the range 0 to 1 which is the output of this subroutine.

The SUBROUTINE RANDU (IX, IY, UNIT) is shown as follows:

```

IY=IX*65539
IF(IY)5,6,6
5 IY=IY+2147483647+1
6 UNIT = IY
UNIT = UNIT*.4656613E-9
RETURN
END

```

By use of the time interval distribution $UNIT = e^{-\bar{a}t_i}$ or $t_i = -\frac{\ln(UNIT)}{\bar{a}}$ where \bar{a} is the average rate taken here as 1 count/ms, a sequence of the random time interval $\{t_i\}$ could be generated. t_i stands for the time interval between the i th and the $(i+1)$ th counts. From this $\{t_i\}$ sequence, number of

counts, X_m can be produced. X_m is the number of counts each characterized by t_j which satisfies the following relation

$$M-1 < \sum_{i=1}^j t_i \leq m \quad (28)$$

Where m represents integers which have to be greater than 1. In other words, X_m is equal to j under the equation (28).

Physically, t_i is the time interval between two consecutive events. The simulated random datum X_m is the number of events between a particular time m and $m + \Delta t$ where $\Delta t = 1$ ms. Note the average time interval between events (counts) is also 1 ms.

X_m is nothing but the number of 'Addition'. This technique can be completed by a 'DO' loop (see Figure 16, blocks 18 and 19) and a testing statement (see Figure 16, block 20). These X_m data are stored in a nine track tape with 800 bits/inch and with the form of variable record length. There are 100 records in this tape and each record stores 1000 numbers of data.

For the purpose of checking X_m and t_i , 10th, 20th, 30th ... 100th's record of data are printed out by use of the 'Mod' function (see Figure 16 block 23) and testing statement (see Figure 16, block 24).

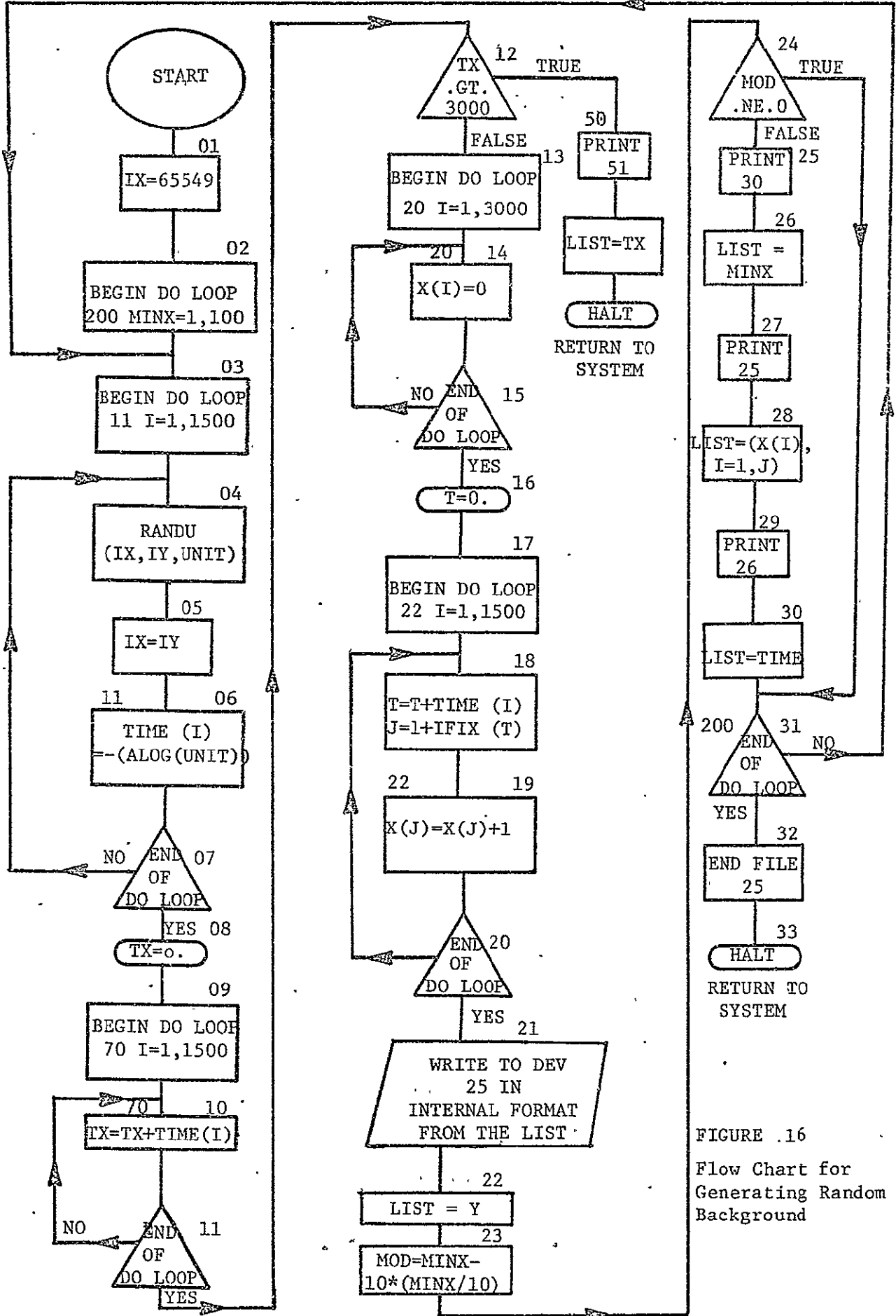


FIGURE .16
Flow Chart for
Generating Random
Background

APPENDIX B

FLOW CHART FOR GENERATING PULSAR SIGNAL ABOVE THE RANDOM BACKGROUND

This is almost the same as in the case of the random background, except it calls for using the RANDU SUBROUTINE twice. The random times t_i and Q_t_i were generated for counting rates of 1ct/ms, and 2cts/ms respectively. Using the same transformation as before, from Q_t_i to Q_i , which corresponds to X_m above, gives a signal with intensity of 100% increase over the random background. However, a periodic signal above the random background can be generated by substituting Q_i for the particular values of X_m . The width of the signal and its period will determine these particular numbers of X_m to be substituted. In Figure 17, blocks 43, 44, 45 and 46, I = 35, 1000, 40; J = 1, 5; K = K + 1; X(I + J) = Q(K) shows the method by which a pulsar signal above background can be produced, i.e. this pulsar signal would have an on time of 5 ms and an off-time of 35 ms. Similarly, if I = 20, 1000, 40; J = 1, 20 statements correspond to a square pulse signal with the same period (40 ms). This signal has an off-time of 20 ms and an on-time of 20 ms.

In order to test the sum of X_m in each record an additional variable M (where $M = \sum_{m=1}^{1000} X_m$) must be considered. This could be printed out along with X_m and t_i every 10th record.

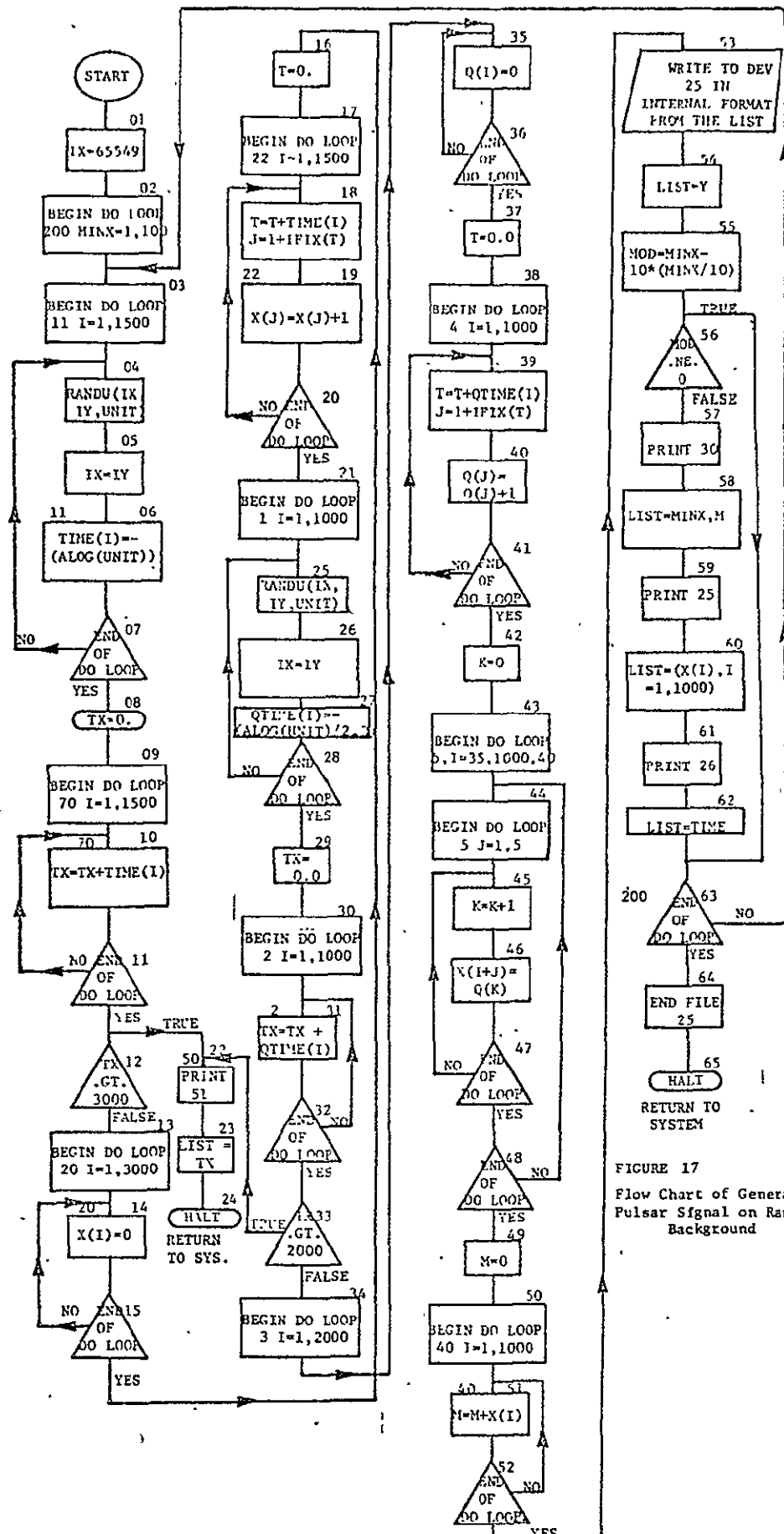


FIGURE 17
Flow Chart of Generating Pulsar Signal on Random Background

FIGURE 17

APPENDIX C

PROGRAMS

There are five programs in this appendix: (1) the program of generating random background, (2) the program of generating square pulse signal with 100% intensity above random background, (3) the program of generating pulsar type signal with 100% intensity above random background, (4) the program of generating pulsar signal with 25% intensity above random background, and (5) the program of calculating autocorrelation function and power spectrum.

The Program of Generating Random Background

FORTRAN IV G LEVEL 18

MAIN

DATE = 70285

```

0001      DIMENSION TIME(1500),X(3000),R(105),Y(1000)
0002      INTEGER*4 X,Y
0003      EQUIVALENCE (X,Y)
0004      IX=65549
0005      DO 200 MINX=1,100
0006      DO 11 I=1,1500
0007      CALL RANDU(IX,IY,UNIT)
0008      IX=IY
0009      11 TIME(I)=-ALOG(UNIT)
0010      TX=0.
0011      DO 70 I=1,1500
0012      70 TX=TX+TIME(I)
0013      IF(TX.GT.3000.)GO TO 50
0014      DO 20 I=1,3000
0015      20 X(I)=0
0016      T=0.
0017      DO 22 I=1,1500
0018      T=T+TIME(I)
0019      J=1+IFIX(T)
0020      22 X(J)=X(J)+1
0021      WRITE(25) Y
0022      MOD=MINX-10*(MINX/10)
0023      IF(MOD.NE.0) GO TO 200
0024      PRINT 30,MINX
0025      30 FORMAT('IMINX= ',I5)
0026      PRINT 25, (X(I),I=1,J)
0027      25 FORMAT('1',/(1X,10I10))
0028      PRINT 26,TIME
0029      26 FORMAT('TIME',/(1X,10F10.3))
0030      200 CONTINUE
0031      END FILE 25
0032      STOP
0033      50 PRINT 51,TX
0034      51 FORMAT(' TX IS ',I8)
0035      STOP
0036      END

```

With 100% Intensity Above Random Background

TRAN IV G LEVEL 19

MAIN

DATE = 71062

19

```

01      DIMENSION TIME(1500),X(3000),R(105),Y(1000)
02      DIMENSION QTIME(1000),Q(2000)
03      INTEGER*4 X,Y
04      INTEGER*4 Q
05      EQUIVALENCE (X,Y)
06      IX=65549
07      DO 200 MINX=1,100
08      DO 11 I=1,1500
09      CALL RANDU(IX,IY,UNIT)
10      IX=IY
11      TIME(I)=- ALOG(UNIT)
12      TX=0.
13      DO 70 I=1,1500
14      TX=TX+TIME(I)
15      IF(TX.GT.3000.)GO TO 50
16      DO 20 I=1,3000
17      X(I)=0
18      T=0.
19      DO 22 I=1,1500
20      T=T+TIME(I)
21      J=1+IFIX(T)
22      X(J)=X(J)+1
23      DO 1 I=1,1000
24      CALL RANDU(IX,IY,UNIT)
25      IX=IY
26      QTIME(I)=- ALOG(UNIT)/2.0
27      TX=0.0
28      DO 2 I=1,1000
29      TX=TX+QTIME(I)
30      IF (TX.GT.2000.) GO TO 50
31      DO 3 I=1,2000
32      Q(I)=0
33      T=0.0
34      DO 4 I=1,1000
35      T=T+QTIME(I)
36      J=1+IFIX(T)
37      Q(J)=Q(J)+1
38      K=0
39      DO 5 I=20,1000,40
40      DO 5 J=1,20
41      K=K+1
42      X(I+J)=Q(K)
43      M=0
44      DO 40 I=1,1000
45      M=M+X(I)
46      WRITE (25) Y
47      MOD=MINX-10*(MINX/10)
48      IF(MOD.NE.0) GO TO 200

```

FORTRAN IV G LEVEL 19

MAIN

DATE = 71062

```
049      PRINT 30,MINX,M
050      30 FORMAT ('1MINX= ',I5,/, ' M= ',I5)
051      PRINT 25, (X(I),I=1,1000)
052      25 FORMAT('1',/(1X,10I10))
053      PRINT 26,TIME
054      26 FORMAT('TIME',/(1X,10F10.3))
055      200 CONTINUE
056      END FILE 25
057      STOP
058      50 PRINT 51,TX
059      51 FORMAT(' TX IS ',I8)
060      STOP
061      END
```

The Program of Generating Pulsar Type Signal

With 100% Intensity Above Random Background

FORTRAN IV G LEVEL 19 MAIN DATE = 71047

```

0001      DIMENSION TIME(1:500),X(3000),R(105),Y(1000)
0002      DIMENSION QTIME(300),Q(600)
0003      INTEGER*4 X,Y
0004      INTEGER*4 Q
0005      EQUIVALENCE (X,Y)
0006      IX=65549
0007      DO 200 MINX=1,100
0008      DO 11 I=1,1500
0009      CALL RANDU(IX,IY,UNIT)
0010      IX=IY
0011      11 TIME(I)=-ALOG(UNIT)
0012      TX=0.
0013      DO 70 I=1,1500
0014      70 TX=TX+TIME(I)
0015      IF(TX.GT.3000.)GO TO 50
0016      DO 20 I=1,3000
0017      20 X(I)=0
0018      T=0.
0019      DO 22 I=1,1500
0020      T=T+TIME(I)
0021      J=1+IFIX(T)
0022      22 X(J)=X(J)+1
0023      DO 1 I=1,300
0024      CALL RANDU(IX,IY,UNIT)
0025      IX=IY
0026      1 QTIME(I)=-ALOG(UNIT)/2.0
0027      TX=0.0
0028      DO 2 I=1,300
0029      2 TX=TX+QTIME(I)
0030      IF (TX.GT.600.0). GO TO 50
0031      DO 3 I=1,600
0032      3 Q(I)=0
0033      T=0.0
0034      DO 4 I=1,300
0035      T=T+QTIME(I)
0036      J=1+IFIX(T)
0037      4 Q(J)=Q(J)+1
0038      K=0
0039      DO 5 I=35,1000,40
0040      DO 5 J=1,5
0041      K=K+1
0042      5 X(I+J)=Q(K)
0043      M=0
0044      DO 40 I=1,1000
0045      40 M=M+X(I)
0046      WRITE (25) Y
0047      MOD=MINX-10*(MINX/10)
0048      IF(MOD.NE.0) GO TO 200

```

FORTRAN IV G LEVEL 19

MAIN

DATE = 71047

2

```
249      PRINT 30,MINX
250 30 FORMAT ('1MINX= ',15)
251      PRINT 27, M
252 27 FORMAT ('M= ',I10)
253      PRINT 25, (X(I),I=1,1000)
254 25 FORMAT('1',/(1X,10I10))
255      PRINT 26,TIME
256 26 FORMAT('TIME',/(1X,10F10.3))
257 200 CONTINUE
258      END FILE 25
259      STOP
260 50 PRINT 51, TX
261 51 FORMAT(' TX IS ',I8)
262      STOP
263      END
```

With 25% Intensity Above Random Background

STRAN IV G LEVEL 19

MAIN

DATE = 71092

22/

```

001      DIMENSION TIME(1500),X(3000),R(105),Y(1000)
002      DIMENSION QTIME(1000),Q(2000)
003      INTEGER*4 X,Y
004      INTEGER*4 Q
005      EQUIVALENCE (X,Y)
006      IX=65549
007      DO 200 MINX=1,100
008      DO 11 I=1,1500
009      CALL RANDU(IX,IY,UNIT)
010      IX=IY
011      11 TIME(I)=-ALOG(UNIT)
012      TX=0.
013      DO 70 I=1,1500
014      70 TX=TX+TIME(I)
015      IF(TX.GT.3000.)GO TO 50
016      DO 20 I=1,3000
017      20 X(I)=0
018      T=0.
019      DO 22 I=1,1500
020      T=T+TIME(I)
021      J=1+IFIX(T)
022      X(J)=X(J)+1
023      DO 1 I=1,1000
024      CALL RANDU(IX,IY,UNIT)
025      IX=IY
026      1 QTIME(I)=-ALOG(UNIT)/1.25
027      TX=0.0
028      DO 2 I=1,1000
029      2 TX=TX+QTIME(I)
030      IF (TX.GT.2000.) GO TO 50
031      DO 3 I=1,2000
032      3 Q(I)=0
033      T=0.0
034      DO 4 I=1,1000
035      T=T+QTIME(I)
036      J=1+IFIX(T)
037      4 Q(J)=Q(J)+1
038      K=0
039      DO 5 I=35,1000,40
040      DO 5 J=1,5
041      K=K+1
042      5 X(I+J)=Q(K)
043      M=0
044      DO 40 I=1,1000
045      40 M=M+X(I)
046      WRITE (25) Y
047      MOD=MINX-10*(MINX/10)
048      IF(MOD.NE.0) GO TO 200

```

TRAN IV G LEVEL 19

MAIN

DATE = 71092

22/

```
49      PRINT 30,MINX,M
50 30 FORMAT ('1MINX= ',I5,/, ' M= ',I5)
51      PRINT 25, (X(I),I=1,1000)
52 25 FORMAT('1',/(1X,10I10))
53      PRINT 26,TIME
54 26 FORMAT('TIME',/(1X,10F10.3))
55 200 CONTINUE
56      END FILE 25
57      STOP
58 50 PRINT 51,TX
59 51 FORMAT(' TX IS ',I8)
60      STOP
61      END
```

and Power Spectrum

AN IV G LEVEL 19

MAIN

DATE = 71095

03/44

```

DIMENSION X(1000),Y(1000),A(1000),R(100),S(100),U(100),V(100),
*COSINE(199),RR(100)
COMMON /TSAI/X,Y
INTEGER*4 X,Y,A,S,R,AVER
EQUIVALENCE(X(501),A(1))
C CALCULATE INITIAL CCRRECTION
N=100
READ (25) X
S(1)=0
R(1)=0
DO 1 I=2,N
S(I)=0
R(I)=0
K=I-1
DO 1 J=1,K
1 S(I)=S(I)+X(J)
AVER=0
NUMBER=0
DO 2 I=1,500
AVER=AVER+X(I)
DO 2 J=1,N
2 R(J)=R(J)+X(I)*X(I+J-1)
NUMBER=NUMBER+500
C MAIN LOOP
3 READ (25,END=6) Y
DO 4 I=1,1000
AVER=AVER+A(I)
DO 4 J=1,N
4 R(J)=R(J)+A(I)*A(I+J-1)
NUMBER=NUMBER+1000
DO 5 I=1,1000
5 X(I)=Y(I)
GO TO 3
C FINISH CALCULATION FOR LAST RECORD
6 DO 7 I=1,500
7 AVER=AVER+A(I)
NUMBER=NUMBER+500
AVE=FLOAT(AVER)/FLOAT(NUMBER)
AVE2=AVE*AVE
DO 8 J=1,N
K=501-J
DO 8 I=1,K
8 R(J)=R(J)+A(I)*A(I+J-1)
DO 9 J=2,N
K=502-J
DO 9 I=K,500
9 S(J)=S(J)+A(I)
DO 10 J=1,N

```

FORTRAN IV G LEVEL 19

MAIN

DATE = 71095

```

0045      10 RR(J)=(R(J)+S(J)*AVE-AVE2*(NUMBER+J-1))/(NUMBER-J+1)
0046      PRINT 51,NUMBER,AVER,AVE2,R,S
0047      51 FORMAT (2X,2I15,F20.10,/(2X,8I15))
C      CALCULATE SPECTRAL DENSITY
0048      PI=3.14159265358979
0049      DO 12 I=0,198
0050      12 COSINF(I+1)=COS(I*PI/99.0)
0051      DO 13 K=1,N
0052      KL=MOD(K,2)
0053      KM=MOD(K+1,2)
0054      V(K)=2.0*(RR(1)+KL*RR(100)-KM*RR(100))
0055      DO 13 L=2,99
0056      M=(L-1)*(K-1)
0057      IF(M.GT.198) M=MOD(M,198)
0058      13 V(K)=V(K)+RR(L)*COSINE(M+1)*4.0
0059      U(1)=0.5*(V(1)+V(2))
0060      DO 14 I=2,N
0061      14 U(I)=C.25*V(I-1)+0.5*V(I)+0.25*V(I+1)
0062      U(100)=0.5*(V(99)+V(100))
0063      PRINT 50,((I,RR(I),V(I),U(I),I=1,N))
0064      50 FORMAT('1',/,4X,'I',9X,'R',11X,'V',11X,'U',//,/(2X,I5,3
* (2X,F20.8)))
0065      STOP
0066      END

```

APPENDIX D

CALCULATIONS OF THE POWER RATIOS

The power contributed by each frequency component is proportional to the square of its amplitude. It may be calculated from the area under the curve of the relevant portion of the power spectrum i.e. that area bounded by the curve of the spectrum between specified frequency limits and the estimated mean level of the noise background.

The large value peaks were analyzed in this fashion. Each peak was formed from three consecutive frequencies. This was because the data had been obtained in a digital form.

In this experiment the estimated magnitude of the power of the noise in each frequency component was obtained from the mean power for the frequencies 250 ~ 495 HZ. This was calculated to be $3.008 \text{ (counts}^2/\text{HZ)}$ for Table 3 and $2.248 \text{ (counts}^2/\text{HZ)}$ from Table 4.

For square pulse signals above a random background, the power ratio of the fundamental component to the first harmonic component is 9/1 and that of the fundamental component to the second harmonic component is 25/1. These values were calculated as 8.558/1 and 25.349/1.

The pulsar analysis gives power ratios of the fundamental frequency to the second harmonic component to be 1.57/1 and that of the first component to the third as 2/1. The calculated obtained values were 1.47/1 and 1.81/1.